Intercomparison of global foliar trait maps reveals fundamental differences and limitations of upscaling approaches

B. Dechant[1,2], J. Kattge[3,1], R. Pavlick[4], F.D. Schneider[4], F.M. Sabatini[5,6], A. Moreno[7], E.E. Butler[8], P.M. van Bodegom[9], H. Vallicrosa[10,11,12], T. Kattenborn[13,1], C.C.F. Boonman[14], N. Madani[15,4], I.J. Wright[16,17], N. Dong[18,19], H. Feilhauer[13,1], J. Penuelas[11,12], J. Sardans[11,12], J. Aguirre-Gutierrez[20], P.B. Reich[21,8,16] P.J. Leitão[13,1], J. Cavender-Bares[22], I.H. Myers-Smith[23], S.M. Duran[24], H. Croft[25], I.C. Prentice[18,17,26], A. Huth[27,28,1], K. Rebel[29], S. Zaehle[3], I. Simova[30,31], S. Diaz[32,33], M. Reichstein[3,1], C. Schiller[34], H. Bruelheide[35,1], M. Mahecha[13,1], C. Wirth[36,3], Y. Malhi[20], P.A. Townsend[4,37].

Corresponding author: B. Dechant: benjamin.dechant@idiv.de

Twitter: @DechantBenjamin

[1] German Centre for Integrative Biodiversity Research (iDiv) Halle-Jena-Leipzig, Puschstr. 4, D-04103 Leipzig, Germany

[2] Leipzig University, Ritterstraße 26, 04109 Leipzig, Germany

[3] Max Planck Institute for Biogeochemistry, Hans Knöll Str. 10, 07745 Jena, Germany

[4] Jet Propulsion Laboratory, California Institute of Technology, 4800 Oak Grove Drive, Pasadena, CA 91109, USA.

[5] BIOME Lab, Department of Biological, Geological and Environmental Sciences (BiGeA), Alma Mater Studiorum University of Bologna, Via Irnerio 42, Bologna, 40126, Italy.

[6] Czech University of Life Sciences Prague, Faculty of Forestry and Wood Sciences, Kamýcká 129, 165 21 Praha Suchdol, Czech Republic

[7] Image Processing Laboratory (IPL), Universitat de Valéncia, Valencia, Spain

[8] Department of Forest Resources, University of Minnesota, 1530 Cleveland Ave N, St. Paul, MN 55108

[9] Institute of Environmental Sciences, Leiden University, Einsteinweg 2, 2333 CC Leiden, the Netherlands

[10] Department of Civil and Environmental Engineering, Massachusetts Institute of Technology, Cambridge, MA, USA

[11] CSIC, Global Ecology Unit CREAF-CSIC-UAB, Bellaterra, Barcelona 08913, Catalonia, Spain.

[12] CREAF, 08913 Cerdanyola del Vallès, Barcelona 08913, Catalonia, Spain.

[13] Remote Sensing Centre for Earth System Research (RSC4Earth), Leipzig University and Helmholtz Centre for Environmental Research, Talstr. 35, 04103 Leipzig, Germany

[14] Center for Biodiversity Dynamics in a Changing World (BIOCHANGE) and Section for Ecoinformatics & Biodiversity, Department of Biology, Aarhus University, Ny Munkegade 114, 8000 Aarhus C, Denmark

[15] UCLA Joint Institute for Regional Earth System Science and Engineering. 4242 Young Hall, 607 Charles E. Young Drive East, Los Angeles, CA 90095, USA.

[16] Hawkesbury Institute for the Environment, Western Sydney University, Locked Bag 1797, Penrith, NSW 2751, Australia

[17] School of Natural Sciences, Macquarie University, NSW 2109, Australia

[18] Georgina Mace Centre for the Living Planet, Department of Life Sciences, Imperial College London, Silwood Park Campus, Buckhurst Road, Ascot, SL5 7PY, UK;

[19] Department of Biological Sciences, Macquarie University, North Ryde, NSW 2109, Australia.

[20] Environmental Change Institute, School of Geography and the Environment, University of Oxford, Oxford, UK

[21] Institute for Global Change Biology, and School for the Environment and Sustainability, University of Michigan, Ann Arbor, MI 48109, United States

[22] Department of Ecology, Evolution and Behavior, University of Minnesota, 1479 Gortner Ave., Saint Paul, MN 55108

[23] School of GeoSciences, University of Edinburgh, Edinburgh, EH9 3FF, UK

[24] Department of Forest and Rangeland Stewardship, Colorado State University, Fort Collins, Colorado, USA.

[25] School of Biosciences, University of Sheffield, Sheffield, S10 2TN, UK

[26] Ministry of Education Key Laboratory for Earth System modeling, Department of Earth System Science, Tsinghua University, Beijing 100084, China.

[27] Helmholtz Centre for Environmental Research - UFZ, Permoserstr. 15, 04318 Leipzig, Germany

[28] University of Osnabrück, Barbarastraße 12, 49076 Osnabrück, Germany

[29] Copernicus Institute of Sustainable Development, Environmental Sciences, Faculty of Geosciences, Utrecht University, Utrecht, The Netherlands;

[30] Center for Theoretical Study, Charles University, Husova 4, 110 00 Prague, Czech Republic

[31] Department of Ecology, Faculty of Science, Charles University, Viničná 7, 128 44 Prague, Czech Republic

[32] Consejo Nacional de investigaciones Científcas y Técnicas, Instituto Multidisciplinario de Biología Vegetal (IMBIV), Córdoba, Argentina

[33] Facultad de Ciencias Exactas, Físicas y Naturales, Universidad Nacional de Córdoba, Casilla de Correo 495, 5000, Córdoba, Argentina

[34] Institute of Geographical Sciences, Free University Berlin, Malteserstraße 74-100, 12249 Berlin

[35] Institute of Biology/Geobotany and Botanical Garden, Martin Luther University Halle-Wittenberg, Am Kirchtor 1, 06108, Halle, Germany

[36] Institute of Systematic Botany and Functional Biodiversity, Leipzig University, Leipzig, Germany.

[37] University of Wisconsin, Madison, WI, USA.

Abstract

Foliar traits such as specific leaf area (SLA), leaf nitrogen (N) and phosphorus (P) concentrations play an important role in plant economic strategies and ecosystem functioning. Various global maps of these foliar traits have been generated using statistical upscaling approaches based on in-situ trait observations.

Here, we intercompare such global upscaled foliar trait maps at 0.5° spatial resolution (six maps for SLA, five for N, three for P), categorize the upscaling approaches used to generate them, and evaluate the maps with trait estimates from a global database of vegetation plots (sPlotOpen). We disentangled the contributions from different plant functional types (PFTs) to the upscaled maps and calculated a top-of-canopy-weighted mean (TWM) and the community-weighted mean (CWM) of sPlotOpen trait estimates.

We found that the global foliar trait maps of SLA and N differ drastically and fall into two groups that are almost uncorrelated (for P only maps from one group were available). The primary factor explaining the differences between these groups is the use of PFT information combined with land cover products in one group while the other group relied only on environmental predictors. The impact of using TWM or CWM on spatial patterns is considerably smaller than that of including PFT and land cover information. The maps that used PFT and land cover information exhibit considerable similarities in spatial patterns that are strongly driven by land cover. The maps not using PFTs show a lower level of similarity and tend to be strongly driven by individual environmental variables.

Overall, the maps using PFT and land cover information better reproduce the between-PFT trait differences and trait distributions of the *plot*-level sPlotOpen data, while the two groups performed similarly in capturing within-PFT trait variation. Upscaled maps of both groups were moderately correlated to *grid-cell*-level sPlotOpen data (R = 0.2-0.6), but only when accounting for the differences in processing in the upscaling approaches by applying similar scaling to the sPlotOpen data.

Our findings indicate the importance of accounting for within-grid-cell trait variation, which has important implications for applications using existing maps and future upscaling efforts.

Keywords: foliar trait, specific leaf area, leaf nitrogen, leaf phosphorus, global map, upscaling

1. Introduction

Vascular plants play a crucial role in the terrestrial Earth system due to their exchange of carbon, water, nutrients, and energy with the atmosphere and the pedosphere. Moreover, plants are important elements in the biosphere as they are strong drivers of the population dynamics of other organisms. Functional traits are important for characterizing vegetation function and plant ecological strategies related to metrics of performance, such as nutrient retention, biomass accumulation and CO_2 uptake (Wright *et al.*, 2004; Díaz *et al.*, 2015; Bongers *et al.*, 2021). In particular, morphological and chemical leaf traits, such as specific leaf area (SLA) and leaf concentrations of phosphorus (P) and nitrogen (N), are key components of the leaf economic spectrum (Wright *et al.*, 2004). In turn, the leaf economic spectrum contributes to determining plant growth strategies and canopy carbon exchange dynamics globally (Reich, 2014).

Due to their important roles in plant metabolism, the leaf traits N, P and SLA have been used as inputs to land surface models (Walker *et al.*, 2017), but often in highly simplified ways. As there are currently no observations (or more direct estimates) of these key foliar traits at the global scale, most land surface modeling applications use plant functional type (PFT) look-up tables for key traits such as photosynthetic capacity, which is closely related with N, P and SLA (Kattge *et al.*, 2009; Walker *et al.*, 2014). These look-up tables contain PFT mean trait values that can be combined with remote sensing-based maps of land-cover types dominated by particular PFTs to approximate global trait distributions, but these approaches ignore considerable within-PFT trait variability driven by inter- and intraspecific trait variation (Kattge *et al.*, 2011; Van Bodegom *et al.*, 2012; Scheiter *et al.*, 2013). Furthermore, the focus on dominant PFTs detectable by remote sensing emphasizes top-of-canopy vegetation and ignores the complexity of multi-layered ecosystems.

To overcome the limitations of simplified approaches based on PFT mean trait values for land surface modeling applications and to address ecological questions (related to aspects of functional biodiversity), static maps of SLA, N, P and other traits have been produced based on *in-situ*, leaf-level trait measurements using statistical upscaling approaches at regional (Swenson & Weiser, 2010; Šímová *et al.*, 2018; Loozen *et al.*, 2020; Zhang *et al.*, 2021) and global scales (van Bodegom *et al.*, 2014; Butler *et al.*, 2017; Madani *et al.*, 2018; Moreno-Martínez *et al.*, 2018; Boonman *et al.*, 2020; Schiller *et al.*, 2021; Vallicrosa *et al.*, 2021; Wolf *et al.*, 2022). These upscaled maps of N, P and SLA were generated using different methods, different trait databases and were developed for a range of purposes, such as supporting land surface modeling, biodiversity characterization or a trait-based estimation of the distribution of vegetation types. Given these contrasting approaches and aims we sought to understand the

degree of consistency among these maps, as well as their performance when evaluated in comparison to *in-situ* data.

For potential users, the reliability of upscaled global foliar trait maps and their suitability for specific purposes are difficult to assess. Identifying the key sources of uncertainties and limitations of these maps can provide guidance for users and help improve global mapping of plant traits. Here we provide a comprehensive evaluation of the current global upscaled foliar trait maps of SLA, leaf nitrogen concentration (N) and leaf phosphorus concentration (P) consisting of the following elements:

1) Categorization of upscaling approaches;
2) Comparison of spatial patterns and attribution of differences to upscaling methodology;
3) Evaluation against trait estimates based on a global vegetation plot database.

2. Materials and methods

2.1 Terminology

The upscaling of foliar trait maps is relevant for different scientific communities (e.g., land surface modeling, vegetation remote sensing, macroecology), which may use different terms or partly similar terms that have different meanings. To avoid misunderstandings and be able to use convenient shorthand notations for concepts frequently used throughout the manuscript, we clarify our use of key terms with the following definitions (Table 1). We do not claim that these definitions are necessarily optimal or universal, rather, they serve as a pragmatic way to clarify terms used in the presentation of our study. Note that the land cover types (LCTs) we consider are land cover *functional* types in the sense that they can be directly matched to PFTs (Table 2) in the sense used in previous work (Friedl *et al.*, 2002; Poulter *et al.*, 2015).

Table 1: ***Glossary of terms.*** *Key terms used frequently in the manuscript, their abbreviations and intended meaning.*

Plant functional type (PFT)	classification of plants, mostly based on growth form, leaf type and leaf phenology. Example: evergreen needleleaf tree.
Land cover type (LCT)	remote sensing-based classification of the land cover, dominated by specific PFTs. Example: evergreen needleleaf forest.
Community weighted mean (CWM)	the mean trait value of a community weighted by the species cover, abundance, or biomass. In the case of the sPlotOpen dataset the weighting is done by species cover or abundance.
Top-of-canopy weighted mean (TWM)	the mean trait value at the top-of-canopy weighted by the cover of the species that constitute the dominant PFT of a plot.
Homogeneous grid cells	grid cells with low trait variability, either occupied by a single LCT or several LCTs with similar trait values.
Heterogeneous grid cells	grid cells with high trait variability, occupied by more than one dominant PFT with considerable differences in mean trait values of the dominant PFTs.

2.2 Trait maps

We identified seven publications in the literature (state June 2022) that present global, statistically upscaled trait maps with at least one of the three traits SLA, N or P: van Bodegom *et al.* (2014); Butler *et al.* (2017); Madani *et al.* (2018), Moreno-Martínez *et al.* (2018), Boonman *et al.* (2020), Schiller *et al.* (2021), and Vallicrosa et al. (2021) (Table 2). For the sake of simplicity, we use a short version of the last name of the first author of each map-related publication to refer to the different maps, e.g., 'Bodegom' refers to the map of van Bodegom et al. (2014). 'Moreno' refers to Moreno-Martinez et al. (2018) (see Table 2).

The degree of completeness of the spatial coverage of the maps differed. Four maps provided gap-free global maps (Bodegom, Butler, Madani, Boonman), while the two high-resolution maps excluded cropland (Moreno, Vallicrosa). Schiller had gaps in different regions due to the availability/selection of plant photographs from iNaturalist. All upscaling approaches except Madani only considered trait variation in natural vegetation and excluded foliar traits in croplands. While most approaches considered vegetation of different growth forms, Vallicrosa only mapped traits for woody vegetation (Table 2).

Table 2: Overview of key information of the seven upscaling approaches and the corresponding maps. *This includes the short version of the lead author name used in the text, year of publication, the foliar traits covered, whether plant functional type (PFT) information was used or not, the spatial resolution in degrees latitude/longitude, the vegetation types considered and the full first author name of the reference publication. The resolutions 0.5°, 0.05°, and 0.008° correspond to square grid cell sizes of about 50 km, 5 km and 1 km at the equator.*

Lead author	Year	Traits	PFT use	Reso-lution	Vegetation Considered	Reference
Bodegom	2014	SLA	0	0.5 °	Natural	van Bodegom et al. (2014)
Butler	2017	SLA, N, P	1	0.5 °	Natural	Butler et al. (2017)
Madani	2018	SLA	1	0.05 °	All	Madani et al. (2018)
Moreno	2018	SLA, N, P	1	0.008 °	Natural	Moreno-Martínez et al. (2018)
Boonman	2020	SLA, N, P	0	0.5 °	Natural	Boonman et al. (2020)
Vallicrosa	2021	N, P	1	0.008 °	Woody	Vallicrosa et al. (2021)
Schiller	2021	SLA, N	0	0.5 °	Natural	Schiller et al. (2021)

2.3 Upscaling approaches

All approaches derived gridded global trait maps from globally distributed leaf-level *in-situ* observations (Fig. S1). The upscaling approaches can therefore be characterized by two steps of upscaling: (1) leaf to grid scaling, and (2) spatialization, i.e., increasing the spatial coverage from the limited number grid cells with *in-situ* data to the global land surface (Fig. 1). All approaches but one first estimated trait values for reference grid cells from leaf-level trait observations available within those cells (leaf-to-grid scaling). Then, the approaches applied regression-based mapping that established trait-environment relationships for the reference grid cells and applied them to the global vegetated land surface to obtain global maps

(spatialization). Schiller, however, switched the order of the two upscaling steps and first estimated trait values for a large number of iNaturalist photographs of individual plants distributed globally and aggregated these trait values to grid-cell-level in the second step.

There were important differences between the upscaling approaches in essentially all aspects of the upscaling processing chain (Fig. 1). The approaches differed in the motivations, the input data and its processing, the leaf to grid scaling method, and the spatialization including both the choice of predictor variables and regression algorithms (Fig. 1, supplementary Methods M1). The environmental predictors used in the upscaling approaches were mainly related to temperature, solar radiation, water availability and soil characteristics (Tables S1) and came from a variety of climate and soil products (Table S2). Moreno was the only approach that directly used optical reflectance satellite remote sensing data (Table S1). Importantly, there were differences regarding the use of land cover type and PFT information in the different upscaling approaches (Fig. 1), which is relevant for our analyses and was the motivation for the categorization below.

Categorization of upscaling strategies. All maps used environmental predictor information ('Env') in the spatialization step but only some used PFT information in either the leaf-to-grid scaling or the spatialization. Therefore, we use the shorthand notation of 'PFT+Env' vs. 'Env' maps to more generally distinguish the upscaling approaches that used PFT information from those that did not. Note that there are considerable differences in the way PFT information was used in the PFT+Env approaches and that in the case of the Schiller map additional information unrelated to PFTs was used but it is still categorized as 'Env' upscaling approach (Fig. 1). 'PFT+Env' is a shorthand for 'PFT+LCT+Env' as PFT and LCT information was always used together and LCTs are matched to PFTs. In a more general sense, LCTs can be seen as PFT-related information at the grid cell level.

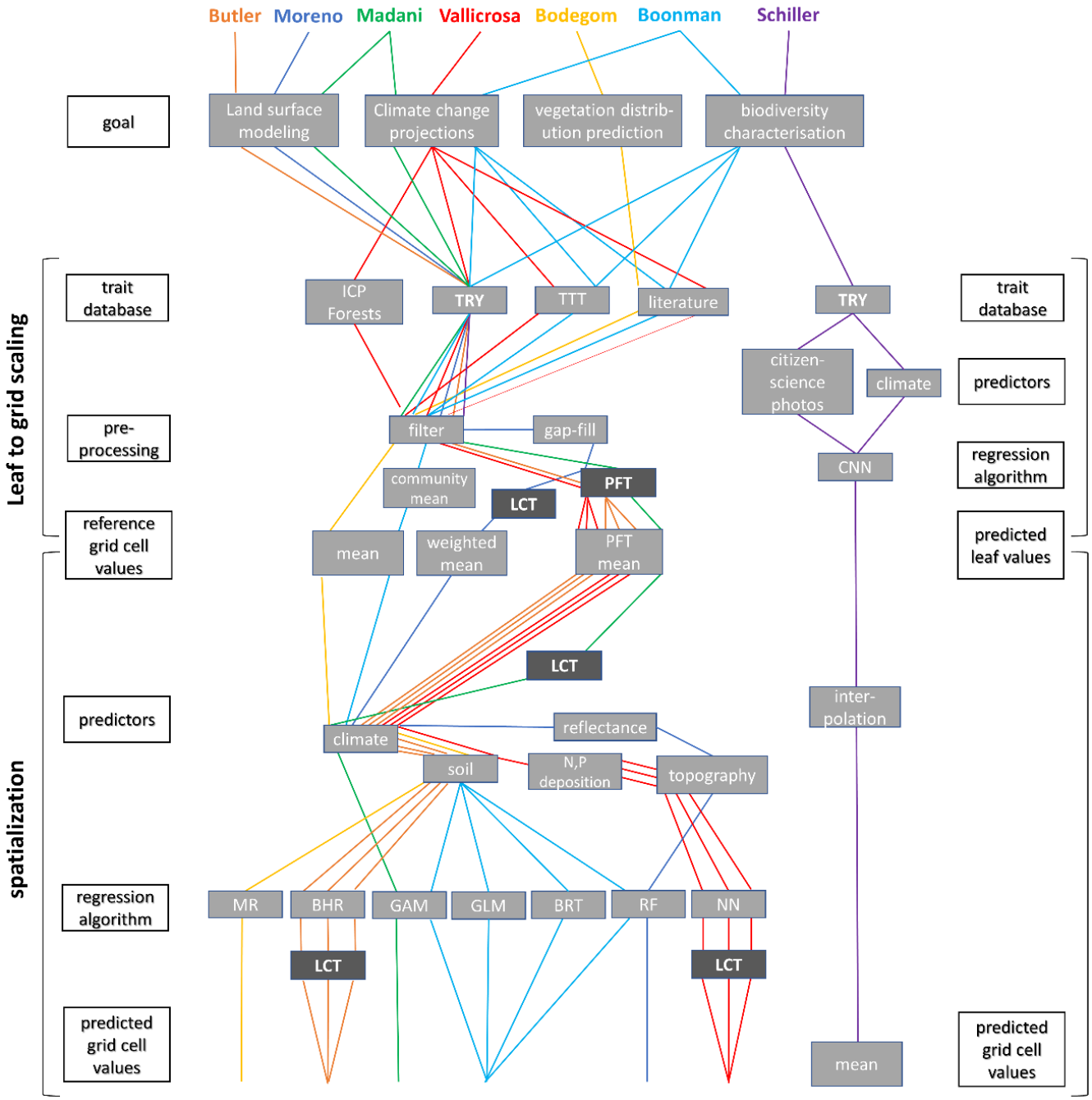

Figure 1: Overview of the seven upscaling approaches in terms of the motivation and the two main upscaling steps as well as their key components. *Each upscaling approach is shown in a separate color connecting the different elements of the upscaling from the motivation and input data at the top to the final predicted grid cell values at the bottom. Special emphasis is put on the use of plant functional type (PFT) and land cover type (LCT) information shown in dark grey color. The explanatory column on the left hand side applies to all approaches except Schiller, while the corresponding column on the right hand side only applies to Schiller. The abbreviations of the trait databases are as follows: 'TTT' refers to the Tundra Trait Team database, 'literature' to data based on individual publications not represented in other trait databases. The abbreviation of the upscaling algorithms are as follows: 'MR' refers to multiple linear regression, 'BHR' to bayesian hierarchical regression, 'GAM' to generalized additive models, 'GLM' to generalized linear models, 'GBM' to generalized boosted models, 'RF' to random forests, 'NN' to neural networks, and 'CNN' to convolutional neural networks. Note that Madani and Vallicrosa used dominant LCT maps, while Moreno and Butler used fractional LCT cover.*

Additional versions of the Butler and Moreno maps. To quantify the relative contributions of different types of predictor information to the upscaled trait maps, we also analyzed versions of the Butler and Moreno trait maps that differed only in the predictor variables used. In particular, Butler produced trait maps with either no PFT categories at all and only environmental drivers (abbreviated as 'Env'), a combination of the two (abbreviated as 'PFT+Env'), and maps that only use LCT cover and mean PFT trait values ('PFT'; 'categorical maps'). We additionally generated an optimized version of the 'PFT' maps by adjusting the PFT mean trait values to match the spatial patterns of the full 'PFT+Env' maps (Fig. S2). In the analyses, we used the optimized maps unless stated otherwise. While for the PFT+Env Butler map we always used the spatial model as it had the best performance in the original publication, for the Env model, we considered both the spatial models including a kriging component and the linear models without this component. Moreno also generated additional trait maps that exclusively used either remote sensing ('RS') or environmental variables ('Env') in the spatialization step (Fig. 1) for comparison to their final map products that combined both types of variables ('RS+Env'). In addition, Moreno generated maps without using PFT information in the leaf-to-grid scaling step.

2.4 Data processing

2.4.1 Global foliar trait maps

We used global trait maps provided by the map developers (the leading authors of the relevant publications) to ensure that we had the most up-to-date and correct versions of the upscaling products. A list of the sources is provided in Table S3. We only used maps representing the present and recent past and did not consider maps of future change predictions such as Madani et al. (2018). We aggregated the higher resolution maps (Madani, Moreno, Vallicrosa) to the common resolution of 0.5 degree using the Bodegom map as reference regarding the projection and coordinate origin. In this aggregation, we used the average over all available high resolution grid cells within a coarse grid cell and ignored missing-data and zero values. Non-vegetated grid cells such as bare soil, ice/snow etc. were excluded. This was done by applying a vegetation cover threshold of 95% on the LCT cover map used by Butler. Madani was the only data set to provide estimates for croplands, so prior to aggregating to 0.5°, we masked out the cropland grid cells at the original resolution of 0.05° using the land cover map used by Madani.

2.4.2 Separation of land cover - driven and environmentally driven trait variation and stratification by PFT

Our initial analyses revealed that LCT cover-driven trait variation dominated the global spatial trait patterns of the PFT+Env maps. To distinguish the LCT cover-driven trait variation, which is related to between-PFT trait differences, from the environmentally driven variation within PFTs, we developed two complementary approaches: filtering homogeneous versus heterogeneous grid cells, and unmixing LCTs in heterogeneous grid cells (see box 1). For analyses at the level of PFTs/LCTs we combined the two approaches to benefit both from the accuracy of the filtering approach and the higher number of available grid-cells of the unmixing approach.

Approach 1: Heterogeneity filtering

Heterogeneity filtering is based on estimates of within grid cell trait variability using LCT cover fractions and differences in average trait values between PFTs corresponding to LCTs. Within-PFT trait variation was explicitly excluded. Higher within grid cell trait variability (a.k.a. heterogeneity) indicates mixing of LCTs with considerable differences in the corresponding mean PFT traits, while lower heterogeneity indicates either dominance of a single LCT or a mixture of different LCTs with similar PFT mean trait values. For this approach, we combined the PFT-mean trait values with global maps of LCT cover fractions for each grid cell, both provided by Butler and originally based on the TRY database (Kattge *et al.*, 2011, 2020) and MODIS and AVHRR satellite products of land cover (Lawrence & Chase, 2007). For each 0.5° grid cell, we then estimated the trait variability by calculating the coefficient of variation (CV) of a variable in which each PFT mean trait value was represented proportional to its LCT cover fraction (Figs. S2). For each trait, we categorized grid cells with higher CV than the median of all grid cells as ‘heterogeneous’ and those with lower CV than the median as ‘homogeneous’.

To stratify the maps by PFT, we combined the heterogeneity filtering with a threshold on the fractional LCT cover. This double threshold approach was necessary because even cells with high cover fraction of one LCT can exhibit high within-grid cell trait heterogeneity due to the mixing of LCTs with strongly differing trait values (Fig. S3b). While the double threshold approach is reasonable for the shrubland (SHR), grassland (GRA), and evergreen broadleaf forest (EBF) LCTs, it has severe limitations for evergreen needleleaf forest (ENF), deciduous needleleaf forest (DNF) and deciduous broadleaf forest (DBF). Specifically, the double threshold filtering does not leave

enough data for robust statistical analyses of ENF, DNF and DBF (Figs. S2c). In case of ENF, this is mainly due to the peak CV located at very high cover fraction (about 0.8), while for DBF the CV peak is at rather low cover fractions (0.2-0.4) but only relatively few grid cells with higher cover fractions exist (Fig. S3b). Therefore, for ENF, DNF and DBF another approach to isolate trait variation related to the corresponding LCT cover was needed.

Approach 2: Unmixing

The second approach entails essentially reverse engineering the final step of calculating grid-cell averages weighted by LCT cover in the generation of some of the 'PFT+Env' trait maps (Fig. 1). While not all maps applied the LCT weighting after the spatialization, this approach can be applied to all maps as the only assumption is the linear mixing of LCTs, i.e. only the spatial distribution of LCT cover is used. The unmixing was done by using a three by three grid cell moving window within which the system of overdetermined linear equations for six PFTs (ENF, DNF, EBF, DBF, SHR, GRA) was solved. For each grid-cell, there is one linear equation that equates the final grid cell trait value (known) with the sum over the six products of fractional LCT cover (known) times the corresponding local, PFT-specific trait value (unknown). For solving the linear equation systems the function *lsei* of the R package *limSolve* was used in combination with the *focal* function of the *terra* package (Van den Meersche *et al.*, 2009; Hijmans *et al.*, 2015; Soetart *et al.*, 2022). We evaluated the performance of the unmixing approach with the categorical maps provided by Butler and found that it performed robustly for ENF and DNF, and reasonably well for DBF and EBF but could not be used for SHR and GRA (Fig. S4a). The limitations for SHR and GRA are likely due to their broad trait distributions and their co-occurrence with other LCTs with similar trait values. To exclude grid cells where the unmixing method did not work well, we applied a threshold on the fractional cover of the relevant PFT of 5% and applied thresholds on the maximum and minimum possible trait values to exclude large outliers or ecologically implausible values. Even after this filtering step, considerably more data were left for analyses of ENF and DBF than in case of applying Approach 1.

Overall approach: combining Approach 1 and Approach 2

Due to the limitations of both approaches for some LCTs, we combined the unmixing approach for ENF, DBF, and EBF with the heterogeneity filtering approach for SHR and GRA. For EBF, both strategies could be used in principle, but we chose to use the unmixing as it provides better data coverage. DNF was excluded from further analyses

due to the sparseness of data from sPlotOpen and the limited geographic extent of the distribution compared to other LCTs.

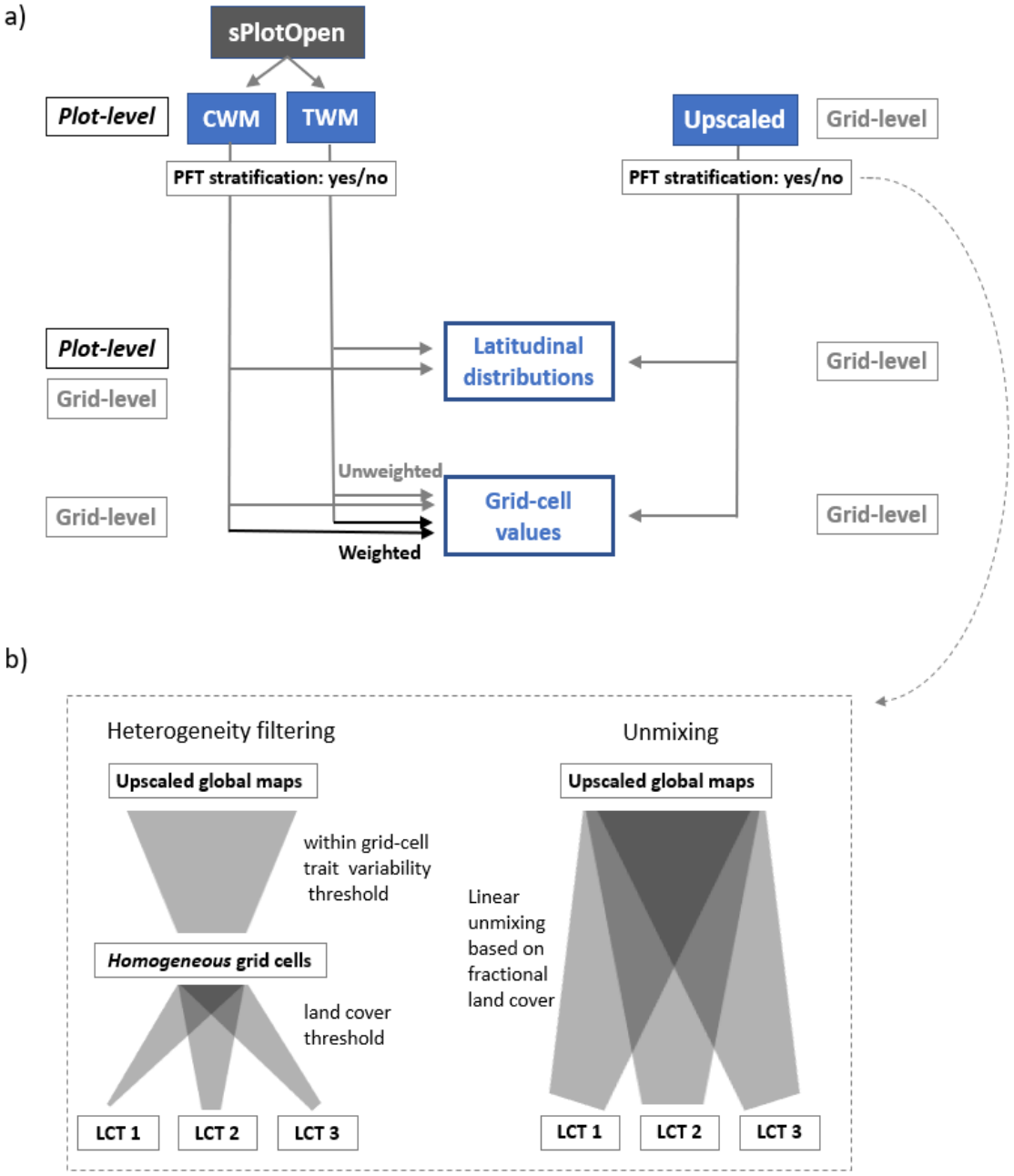

Figure 2: Illustration of the key aspects of the data processing of the upscaled maps and the sPlotOpen reference data. *In a) an overview of the different processing steps and comparisons is shown. For sPlotOpen, either the community weighted mean (CWM) or top-of-canopy-weighted mean (TWM) of sPlotOpen is used and both for sPlotOpen and upscaled maps the data was either stratified by plant functional type (PFT) or not. While upscaled map data is necessarily always at grid-cell level (grid-level), sPlotOpen data can either be used at plot- or grid-level. To obtain grid-level sPlotOpen data, unweighted or land cover type (LCT) fraction-weighted averages can be applied. For upscaled maps, the PFT stratification was done by combining a trait heterogeneity filtering and a linear unmixing approach (b). The heterogeneity filtering approach was based on thresholds on the estimated within grid-cell trait variability (coefficient of variation, CV) and fractional land cover and only suitable for some LCTs.The unmixing approach could be applied to the remaining LCTs.*

2.4.3 Evaluation against sPlotOpen

To evaluate the upscaled maps against data not directly used in the upscaling, we used the sPlotOpen database (Sabatini *et al.*, 2021). sPlotOpen is an open-access collection of 95,104 vegetation plots sampled in the field, spanning 114 countries. It consists of a stratified random selection of vegetation plots derived from sPlot - The Global Vegetation plot database (Bruelheide *et al.*, 2019). Plots vary widely in size, ranging between 0.03 and 40,000 m^2. For each plot, sPlotOpen reports the list of vascular plant species, together with a measure of their relative abundance. Species mean trait values, as extracted from the TRY database (Kattge *et al.*, 2011, 2020), were combined with species abundance data to calculate plot-level community weighted mean (CWM) trait values. To evaluate the impact of vertical variations of foliar traits, we calculated top-of-canopy weight mean (TWM) trait estimates per plot, in addition to the standard CWM trait estimates, which integrate traits from all vegetation layers. This was done by first determining the dominant PFT of each plot using thresholds on the species cover of a given PFT (Table S4) and then calculating the weighted mean over all species of the dominant PFT of the plot. To compare sPlotOpen and upscaled maps at the level of individual PFTs, we stratified both CWM and TWM by PFT by using the dominant PFT of the plot. We used the six PFT categories defined above (ENF, DNF, EBF, DBF, SHR, GRA) and matched the species in sPlotOpen to these categories using plant growth form, leaf type and leaf phenology type from the TRY database and literature.

We compared characteristics of the upscaled maps with sPlotOpen at two levels: using *plot*-level sPlotOpen data and *grid-cell*-level sPlotOpen data (Fig. 2a).

***Plot-level* sPlotOpen data.** The advantage of using plot-level data is that it contains all information of the original observations. These data allow direct comparison of trait distributions. We found that global trait distributions did not contain sufficient (spatial) detail needed for the evaluation, but when calculating trait distributions in latitudinal intervals, meaningful spatial patterns of trait distributions emerged that could be compared.

***Grid-cell-level* sPlotOpen data.** For a grid-cell-level comparison, the sPlotOpen plot data has to be scaled to the grid cell given the fact that sPlotOpen plots are much smaller than the typical grid cell size (50 km). This was done as follows to ensure direct comparability to the upscaled maps. For the comparison to **Env** upscaled maps, we aggregated the plot-level CWMs to the 0.5° grid cells without any weighting. For the comparison to **PFT+Env** upscaled maps, for each PFT, we first aggregated the plot-level TWM data to the 0.5° grid cells without weighting and then combined the six sPlotOpen PFT maps per trait by applying a weighted average based on the fractional LCT cover for each 0.5° grid cell. Data filtering was applied

to ensure that sufficient data from sPlotOpen was available to be reasonably representative of a grid cell by. applying a 99% threshold on the cumulated LCT cover. The high threshold is necessary as small fractions of missing coverage can considerably impact the result if the missing PFT has a very different trait value compared to the other PFTs that are represented, e.g. ENF (Fig. S3b). For the comparison of between- and within-PFT trait variation we used unweighted grid-cell averages of all relevant plots per PFT (with the partial exception of plot-level data in Figs. 9c, S13).

A cross comparison of leaf-to-grid scaling approaches not matching the approaches of the upscaled maps was also included to quantify the impact of such a mismatch on the results.

2.5 Statistical analyses

Principal component analysis (PCA) was used to visualize the grouping and relative correlation of different trait maps. Variables were centered and scaled to unit variance for PCA. Pearson correlation (R) was used to quantify the similarity between two given maps. Apart from the 'normal' correlation based on all selected grid cells, we also quantified the degree of 'local correlation' by calculating correlations in a moving window of 3 × 3 grid cells to quantify the similarity in spatial patterns at smaller scales. For each pair of maps, the local correlation produces a correlation map and to summarize that map, the median was used.

All analyses and image processing were conducted using R version 4.0.2 (R Core Team, 2012), primarily with the *raster* package (Hijmans, 2022).

3. Results

3.1 Intercomparison of global maps and attribution of differences

A visual comparison of the different maps for SLA, N and P indicated substantial differences between the maps for each trait but no obvious grouping or similarities at first sight (Figure S5).

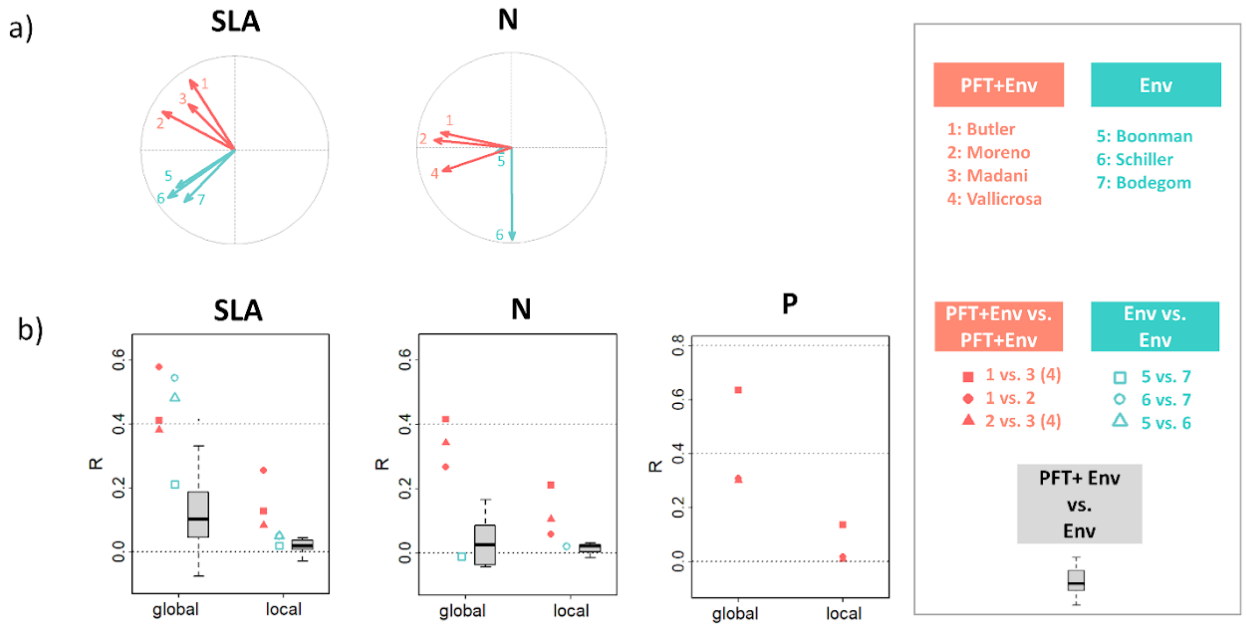

Figure 3: Overview of principal component analyses and pairwise correlation of upscaled maps for specific leaf area (SLA), leaf nitrogen (N) and phosphorus (P) concentration. *In the principal component biplots a) and the pairwise correlation plots b), colors correspond to the use of predictor variables ('Env' stands for environmental variables, while 'PFT' stands for plant functional type and land cover type information). Pearson correlation is shown either for all selected grid cells ('global') or as median value of the local spatial correlation map in 3 x 3 pixel windows ('local'). In b) the gray boxplots contain all possible pairs of PFT+Env maps and the Env maps; for the PFT+Env maps, the same symbols are used for the cases 'x vs. 3' and 'x vs. 4', where x is either 1 or 2, since 3 is only available for SLA and 4 only for N and P; note that the symbols for P and the case '1 vs. 2' and '2 vs. 4' are so close that they are hard to distinguish visually.*

3.1.1 Principal components and pairwise correlations - grouping of maps

We found that the maps clustered according to the use of PFT and LCT information for the upscaling of *in-situ* trait information: approaches using this additional information ('PFT+Env') were similar among each other and different from the other approaches that only used environmental predictors ('Env') (Fig. 3a). For SLA, the PCA results indicate This effect of using PFT information resulted from the dominant influence of heterogeneous grid cells at the global scale as the separation into two groups was similar both when selecting all grid cells or only heterogeneous grid cells, but disappeared when selecting only homogeneous grid cells (Fig. S6a). The first two axes of the PCA explained 60%-65% of the variance for all data selection cases. The patterns in the PCA biplots were confirmed by pairwise correlation analyses showing a higher degree of within-group correlations for the approaches that used PFT information (Fig. 3b). The local correlations were moderately strong for the PFT+Env category, especially for heterogeneous grid cells, but were zero for the Env category (Fig. S6b). High local correlations between maps from the PFT+Env group coincided with grid cells of high within-cell trait heterogeneity (results not shown). For N, the PCA results were generally similar as for SLA (Fig. 3a) with the difference that the correlations within the Env group were low in homogeneous grid cells, as were the correlations between groups (Fig. S6).

The first two axes of the PCA explained 50%-60% of the variance for all data selection cases. For P, only maps based on the use of PFT information were available. They showed similar global pairwise correlations as for SLA, but higher values for the homogeneous grid cells and slightly lower local correlation when all or the heterogeneous grid cells were selected (Fig. 3b).

The impact of using PFT and land cover information on the upscaled maps was so dominant that maps only using this information combined with fixed trait values per PFT ('categorical' or 'PFT' maps) showed similar spatial patterns and fell into the same group of maps as those that also used environmental predictors (Figs. S2, S7a,c).

3.1.2 Global maps: spatial patterns and within-group differences

We grouped the maps according to the use of PFT information and calculated the trait averages over all maps within a given category as well as the coefficient of variation (CV) for each grid cell as a metric for dissimilarity (Fig. 4). These 'synthesis maps' and corresponding CV maps of SLA and N differed considerably between the PFT+Env and Env groups (Fig. 4). On average the CV values within the PFT+Env group were lower than in the Env group. Despite the higher level of similarity of the PFT+Env maps compared to the Env maps, there were considerable differences between individual PFT+Env maps of all three traits such as the notably higher trait values of the Butler maps at high latitudes (Fig. S5).

The average maps for the PFT+Env and Env categories showed considerable differences in spatial patterns (Fig. 4, 5a). For SLA, the PFT+Env mean map had high values in regions dominated by GRA, and SHR PFTs and a distinct band of low values for ENF (Figs. 4, 5a). The Env mean map, in contrast, showed overall low values in the Southern Hemisphere and a band of higher values in parts of the Northern Hemisphere dominated by GRA and ENF (Figs. 4, 5a). For N, the PFT+Env mean map showed somewhat similar patterns with a band of low values in the ENF dominated areas, while the Env mean map had overall high values with little contrast between the Northern and Southern Hemispheres. Also when looking at Europe in more detail (Fig. 4), the PFT+Env maps for SLA and N showed spatial patterns corresponding to dominant LCTs while the Env maps showed little contrast between dominant LCTs. For P, the mean PFT+Env map showed the lowest values in EBF-dominated regions and clearly lower values in the Southern than the Northern Hemisphere. P had somewhat lower values in the ENF-dominated region compared to the surrounding areas but the contrast was smaller than for SLA and N.

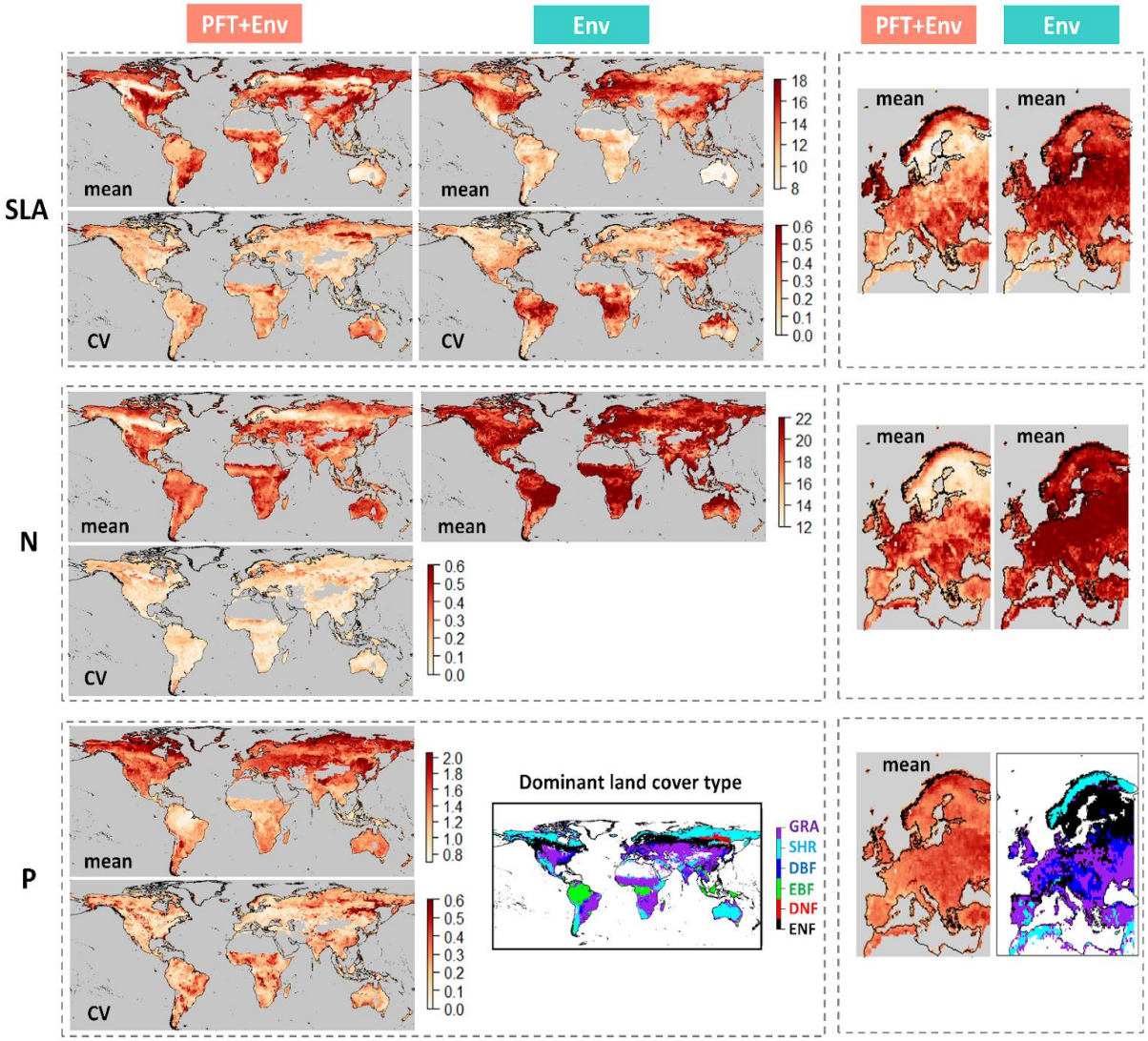

Figure 4: Overview of spatial patterns of specific leaf area (SLA, *mm^2/mg****), leaf nitrogen (N,*** *mg/g****) and phosphorus (P,*** *mg/g****) for different upscaled maps.*** *For each trait, the the upper row shows the average and the lower row shows the coefficient of variation (CV) between the maps of each upscaling category: those that used both plant functional type and environmental information (PFT+Env) and those that use only environmental predictors (Env). The average trait maps for Europe are shown besides the global maps to provide more detailed information on smaller-scale variations. The color scales of the mean maps for Europe are identical to those for the global maps and therefore not shown. The global and European maps of dominant land cover type is shown for reference (ENF: evergreen needleleaf forest; DNF: deciduous needleleaf forest; EBF: evergreen broadleaf forest; DBF: deciduous broadleaf forest; SHR: shrubland; GRA: grassland).*

The higher level of similarity in spatial patterns within the PFT+Env category compared to the Env category was also visible in the latitudinal median patterns of the individual maps (Fig. S8). In particular, the PFT+Env maps showed strongly covarying latitudinal patterns for all three traits despite offsets in absolute values for SLA and divergence at the high northern latitude while Env maps showed very different patterns (Fig. S8). For N, PFT+Env maps showed consistent latitudinal patterns above 25 degree south and divergent patterns below, while Env maps showed the opposite tendency.

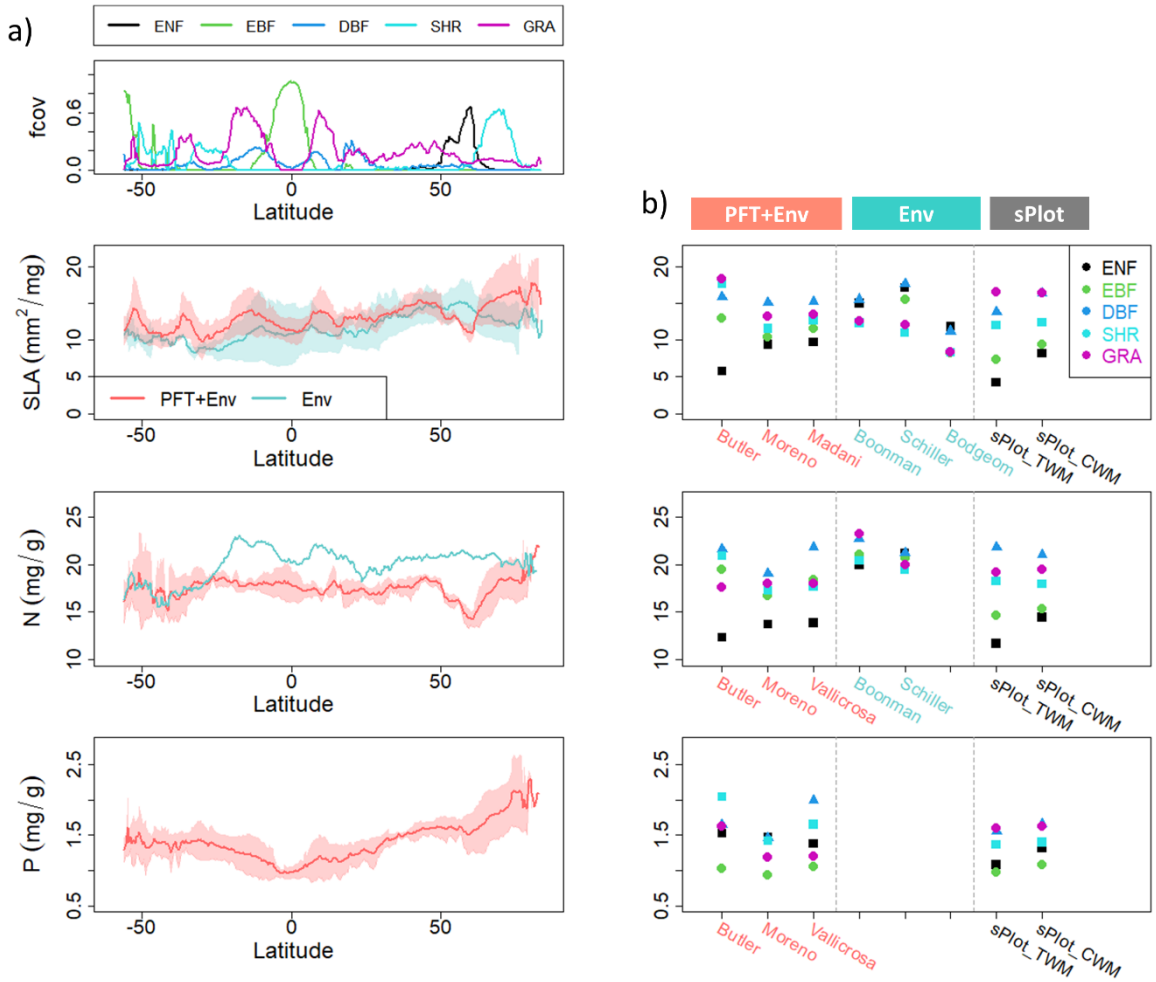

Figure 5: Latitudinal patterns of upscaled trait maps and differences between plant functional types (PFTs). *a) Median latitudinal trait values of fractional PFT cover (fcov) and median latitudinal trait values of specific leaf area (SLA), leaf nitrogen (N) and phosphorus contents (P) averaged over the two upscaling groups (PFT+Env vs. Env). The shading around the mean values indicates one standard deviation (for the N maps with Env approaches there were only two maps, so no standard deviation could be calculated). b) Comparison of mean PFT (fcov > 0.5) trait values per upscaling approach with colors indicating each PFT (ENF: evergreen needleleaf forest; EBF: evergreen broadleaf forest; DBF: deciduous broadleaf forest; SHR: shrubland; GRA: grassland). In contrast to the upscaled maps for which unmixing was used to get median values per PFT, sPlotOpen ('sPlot') was first stratified by PFT and then aggregated to 0.5° grid cells. TWM indicates top-of-canopy data selection, and CWM includes all vertical layers weighted by cover fraction.*

3.2 Evaluation of upscaled global trait maps with sPlotOpen

3.2.1 Comparison to sPlotOpen plot-level data

Latitudinal median values. When reducing the upscaled maps to the grid cells for which sPlotOpen data is available, we found some agreement in the latitudinal patterns of upscaled maps and sPlotOpen plot data (Fig. S11). In particular, the average of the PFT+Env maps agreed well with sPlotOpen data for SLA, N and P in the northern hemisphere including the lower values for ENF (Fig. S11) but the Butler maps showed considerably higher SLA values in the high northern latitudes than sPlotOpen (Figs. S8, S11). In the tropics, PFT+Env maps agreed rather well for SLA and P but showed some discrepancies for N. sPlotOpen generally

showed considerably lower values than upscaled maps in the Southern Hemisphere, with the exception of the Env maps for SLA (Fig. S11). Apart from this exception, Env upscaled maps showed larger discrepancies with sPlotOpen plot data than PFT+Env maps. The latitudinal mean patterns of sPlotOpen trait data only showed rather small differences between TWM and CWM (Fig. S11).

Latitudinal distributions. While latitudinal mean or median values can be a useful way to summarize global patterns, they cannot capture the complexity of multi-modal trait distributions well. The full latitudinal trait distributions of upscaled maps (Fig. 6) partly showed considerable differences compared to sPlotOpen plot data (Fig. 6). Also, there were considerable differences between CWM and TWM distributions, with TWM showing a tendency to broad, multi-modal distributions and CWM a tendency to narrower, unimodal distributions (Fig. 6).

Some of the PFT+Env maps showed considerable similarities with the sPlotOpen TWM distributions with a higher level of agreement for SLA than for N and P (Fig. 6). For SLA, the Butler map best captured the latitudinal patterns of the TWM distribution peaks including the double peak feature in the higher northern latitudes. This double peak feature was also partly captured by the Moreno and Madani maps but with a smaller distance between the peak in case of Moreno and a considerable lower secondary peak in case of Madani. While the Butler and Madani upscaled maps at least partly captured the lower trait values of sPlotOpen TWM at higher latitudes, they did not capture the higher values that also contributed to the overall wider distributions (Fig. 6). For N, PFT+Env upscaled maps did not capture the wide distributions of sPlotOpen TWM in the tropics well. Also, the overall latitudinal patterns of the peaks of the distributions were less consistent between upscaled maps and sPlotOpen TWM than for SLA. For P, the overall latitudinal patterns of PFT+Env upscaled maps was similar to sPlotOpen TWM, but Butler and Moreno maps had considerably narrower distributions than Vallicrosa and sPlotOpen TWM.

Some of the Env upscaled maps showed considerable similarities to the latitudinal distributions of sPlotOpen CWM also with a higher level of similarities for SLA than for N (Fig. 6). For SLA, the Schiller map best captured the patterns in the sPlotOpen CWM data, with general agreement in the patterns of latitudinal peaks. However, neither the Schiller nor the Boonman and Bodegom maps captured the broader distribution of sPlotOpen CWM due to the increasing presence of lower trait values in the higher northern latitudes. For N, the Schiller map agreed better with sPlotOpen CWM than the Boonman map regarding the overall decrease in the peak N values towards higher latitudes. However, the patterns of broader and partly double peaked distributions of sPlotOpen CWM were not captured by the Schiller map

that had narrow, unimodal distributions across the entire latitudinal range. The Boonman map better captured the double peaked distribution of sPlotOpen CWM in the southern hemisphere but showed a decreasing trend towards the higher latitudes.

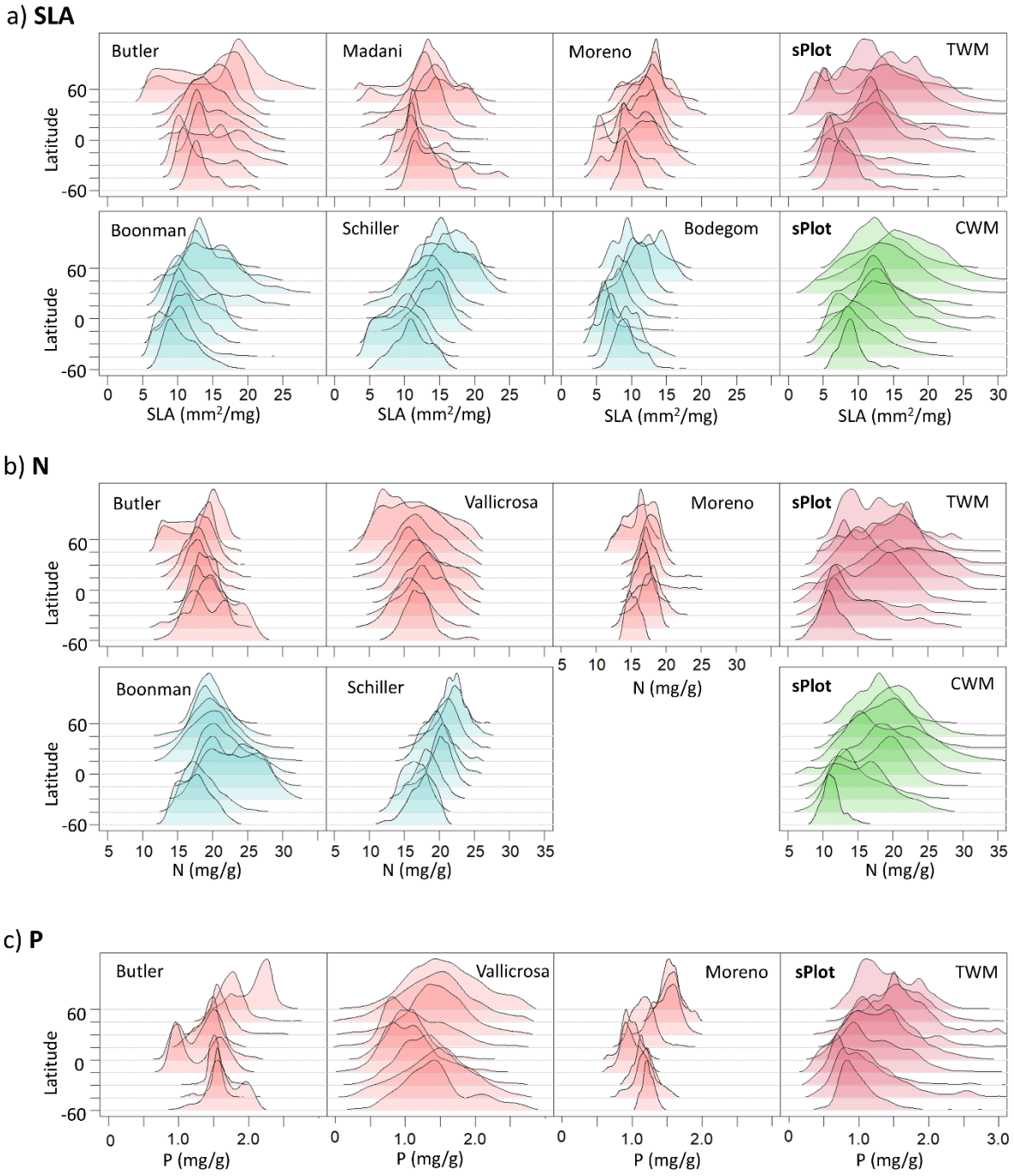

Figure 6: Latitudinal trait distributions for specific leaf area (SLA, *mm²/mg****), leaf nitrogen (N,*** *mg/g****) and phosphorus (P,*** *mg/g****) of upscaled maps and sPlotOpen plot-level data.*** *For each trait, the distributions in latitude intervals (units in degrees) are shown, with the upscaling approaches using plant functional type, land cover and environmental information (PFT+Env) in the top row in red color, and those only using environmental information (Env) in the bottom row. Plot-level sPlotOpen ('sPlot') top-of-canopy weighted mean (TWM) are compared to the PFT+Env maps and community weighted mean (CWM) to the Env maps*

3.2.2 Comparison to sPlotOpen data scaled to the grid level

With PFT stratification

We found considerable differences between upscaled maps in both the spread of trait values between PFTs and the absolute values (Fig. 5b). A general tendency was that the PFT+Env maps showed larger spread between PFTs than the Env maps. This larger spread of the PFT+Env maps was more consistent with grid-level sPlotOpen data for SLA and N than for the Env maps even when considering the difference between top-of-canopy weighted mean (TWM) vs. community weighted mean (CWM). While CWM showed smaller between-PFT differences than TWM, they were still considerable and had mostly similar patterns between PFTs (Fig. 5b). The description of results focuses on mean PFT trait values for the sake of simplicity, but the differences in spread between PFTs can also be observed across latitudinal gradients (Figs. S9, S10).

For SLA, only the Butler map had a similar level of spread between PFTs as sPlotOpen TWM and was the only map that came close to matching the low values for ENF (Fig. 5b). However, the Butler map had much higher values for SHR than sPlotOpen and EBF was also considerably higher but these discrepancies were due to specific latitudinal ranges and agreement in others was considerably better (Fig. S10). The other two PFT+Env maps (Moreno, Madani) were more consistent with sPlotOpen in terms of the order of PFTs, but had considerably smaller between-PFT differences (even smaller than for CWM). While the Env maps differed somewhat in the absolute values, they generally tended to have the highest values for ENF and the lowest values for SHR and GRA, which was opposed to the patterns in sPlotOpen CWM (Fig. 5b).

For N, the difference in values for ENF among the PFT+Env maps was smaller than for SLA, but the differences in spread between PFTs and the order of PFTs were still considerable (Fig. 5b). Similar to SLA, Butler showed higher values for SHR and EBF than sPlotOpen TWM and showed more similar values for DBF and GRA. As for SLA, Moreno showed a similar order of PFTs as sPlotOpen but even smaller spread than CWM. The Vallicrosa maps showed large differences between ENF and DBF but very similar values for the other PFTs. The two Env maps overall had much smaller spread between PFTs than the other upscaled maps and sPlotOpen.

For P, the Butler and Vallicrosa maps showed larger differences between PFTs than sPlotOpen, while the Moreno map had a more similar level of differences (Fig. 5b). There was little similarity in the absolute values between sPlotOpen and the upscaled maps except for

EBF which consistently had the lowest values for the upscaled maps and sPlotOpen. The difference between TWM and CWM was considerably smaller for P than for SLA and N.

We found partially good agreement in some aspects of the within-PFT trait variation between upscaled maps and sPlotOpen, with different maps showing the strongest agreement with sPlotOpen for any given trait and PFT (Figs. S10). In particular, the Butler maps tended to perform well for forest PFTs, with the largest differences to other maps for ENF. However, the high values of the Butler SLA and P maps for SHR and DBF in the high latitudes disagreed with sPlotOpen that showed either a decrease (SLA) or no strong increase (P). Moreno tended to show better agreement with sPlotOpen for SHR and GRA, especially for SLA. Schiller, an Env approach, showed the strongest agreement to reference products for SHR and GRA for SLA, and overall robust performance for the other PFTs except ENF. There are indications that some of the Env maps show better agreement to the within-PFT variation of CWM than TWM, e.g. for the Boonman trait - PFT pairs of SLA - SHR and N - ENF (Fig. S10b).

We found rather low grid-cell to grid-cell correlations of the upscaled maps vs. sPlotOpen at the level of individual PFTs/LCTs. Moderate to strong correlations only emerged when pooling data from all PFTs/LCTs (Fig. S12). In particular, the Butler maps showed high correlations with the difference to the Moreno map mostly being its lower SLA and N values for ENF. The improved Butler categorical maps showed a similar level of correlation as the PFT+Env map.

Without PFT stratification

Overall, we found that the upscaled maps showed moderate correlations (R up to 0.6) to sPlotOpen when matching the leaf-to-grid scaling of sPlotOpen to that of the upscaled maps (Fig. 7a for PFT+Env maps, Fig. 7b for Env maps). When comparing upscaled maps to sPlotOpen scaled to the grid cell with a different approach than was used in the upscaling approaches, the correlations to sPlotOpen were considerably lower for SLA and N (R = 0.2 - 0.4) (Fig. 7b for PFT+Env maps, Fig. 7a for Env maps). For P, however, there were large differences between the scaling options for the PFT+Env maps but they did not follow the same pattern as for SLA and N except for the Butler Env map. In particular, the highest correlation of PFT+Env maps (Moreno) to sPlotOpen was to CWM without LCT cover weighting.

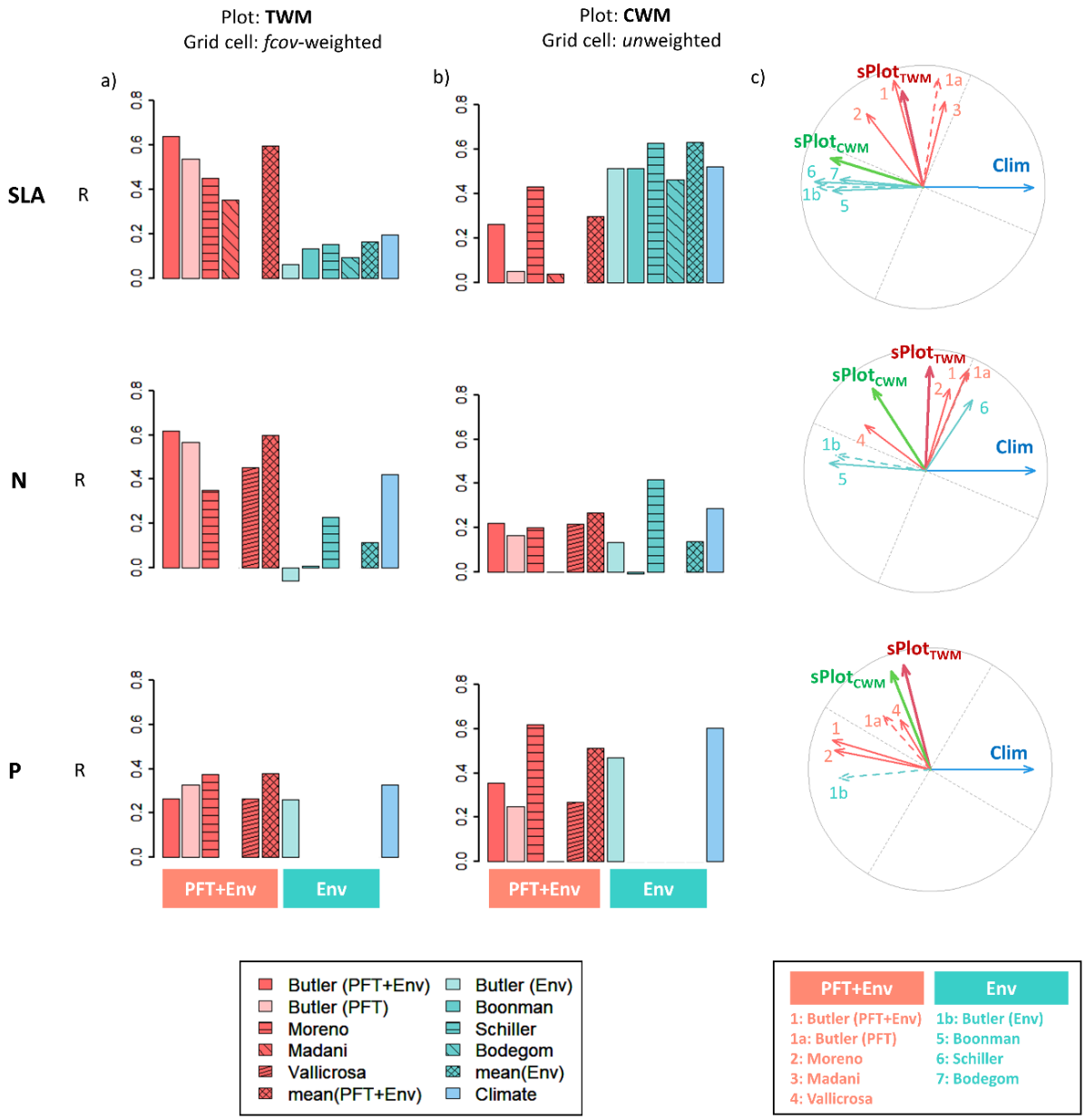

Figure 7: Comparison of upscaled maps against grid-level sPlotOpen data. *The left column a) shows the correlation between upscaled maps against top-of-canopy weighted mean (TWM) sPlotOpen data scaled to the 0.5° grid cell by weighting with the land cover fraction (fcov) corresponding to each plant functional type of the. The middle column b) shows the correlation between upscaled maps and community weighted mean (CWM) sPlotOpen data scaled to the 0.5° grid cell without weighting, i.e. using the unweighted average of all plot-level data within each grid cell. Colors indicate if upscaling maps belong to the group that only used environmental drivers (Env) or additionally used plant functional type (PFT) and land cover information (PFT+Env). The blue colored bars indicate the correlation to sPlotOpen of the single environmental variable (among those used by Butler et al., 2017) with the strongest correlation. The right column c) shows principal component biplots of upscaled maps, sPlotOpen data, and the climate variable (Clim) with the strongest relationships to Env maps (total annual solar radiation for SLA and N, mean annual temperature for P). For sPlotOpen, two processing options corresponding to panels a) and b) are shown in the biplots: sPlot$_{TWM}$ corresponds to a) and sPlot$_{CWM}$ corresponds to b). In a) and b), the mean over the two upscaling groups excludes the different versions of Butler (only PFT, only Env) and the climate cases, i.e. represents the averages over the bars of the corresponding colors. The categorical map (PFT) bar in light red color corresponds to the optimized Butler categorical maps that only used land cover and PFT mean trait values, while the light green bars correspond to the linear version of the Butler maps using only environmental drivers (Env).*

Even when only considering consistent leaf-to-grid scaling of sPlotOpen and the upscaled maps, there were notable differences between individual maps of the upscaling categories (Fig. 7). In the group of PFT+Env maps, the Butler map agreed best with sPlotOpen cover-weighted TWM and the (optimized) categorical map (PFT) showed similar performance as the full upscaled map. The Moreno map showed similar agreement to sPlotOpen cover-weighted TWM as Butler for SLA, but lower correlation for N and higher correlation for P (Fig. 7a). However, the Moreno map tended to agree better with sPlotOpen unweighted (at grid cell level) CWM, with considerable differences for SLA and P and similar correlation for N (Fig. 7b). Among the Env maps, the Schiller map showed consistently better agreement to sPlotOpen unweighted CWM data than the other maps, especially for N (Fig. 7b).

We found a tendency of stronger univariate trait-environment relationships for the unweighted CWM grid cell mean sPlotOpen trait values compared to the LCT cover weighted TWM (Fig. 7). This was most pronounced for SLA and P where a single environmental predictor showed similar levels of correlation to sPlotOpen data aggregated to grid cells without weighting as the 'best' upscaled Env maps.

Due to the complexity of the results, an overview of the key findings and the corresponding results figures is given in Table 3 that can be used alongside the detailed results description above.

Table 3: **Overview of key results and the corresponding figures. '**PFT' stands for plant functional type, 'Env' for environmental predictor variables (climate, soil), 'TWM' for top-of-canopy weighte mean, 'CWM' for community weighted mean, and 'sPlot' refers to sPlotOpen.

Key results	Main figures	Supplementary figures
Two fundamentally different categories of maps/upscaling approaches using only environmental drivers (Env) or additionally PFT and land cover (PFT+Env)	Figs. 1, 3, 4, 5, 6, 7, 8	Fig. S5-S9, S14, S15, S16
PFT+Env maps strongly driven by PFT and land cover due to dominance of between-PFT over within-PFT trait variation; Env maps strongly driven by key environmental drivers	Figs. 4, 7, 8	Fig. S7, S14, S15
Larger between-PFT differences for PFT+Env than for Env maps; Overall PFT+Env more consistent with sPlot for between-PFT, similar performance for within-PFT trait variation	Figs. 5b, 6	Figs. S9, S10, S15
Wide, multi-modal trait distributions for PFT+Env maps and sPlot plot-level TWM vs. narrower, unimodal distributions for Env maps and sPlot plot-level CWM	Figs. 6, 9c	Fig. S13, Fig. S18a
Strong impact of leaf/plot-to-grid scaling on evaluation with sPlot data	Fig. 7a-c	Fig. S17
Impacts of aggregation of in-situ data to grid cells: horizontal weighting with land cover fractions vs. no weighting dominates over vertical weighting (TWM/CWM)	Figs. 7c	S13, S14, Fig. S18b
Most sPlot data are located in heterogeneous grid cells; stratifying by PFT can considerably reduce the within-grid cell trait variability, especially for TWM	Fig. 9a,b	Fig. S17
Impacts of unweighted averaging of in-situ data to grid cells results in strong dependence of resulting trait distributions on grid cell size	Fig. 9c	Fig. S13

4. Discussion

We comprehensively compared seven approaches for the global upscaling of foliar trait data for SLA, and mass based leaf N and P concentrations. For each trait, we found considerable differences between the global maps (Fig. 3, S4) and identified two clearly separated groups of upscaling approaches (Figs 3, 4): one using PFT and land cover information in addition to environmental predictors and one only relying on environmental predictors. Since the use of PFT information explained the main differences between the upscaled maps (despite various other methodological differences), it is important to address the question of what using PFT information versus not using it implies, and what the motivations behind these different approaches are. Also, while there is a close association of using top-of-canopy weight mean (TWM) together with PFT information in the existing upscaled maps, the choice of upscaling TWM or community-weighted mean (CWM) should be considered separately from the use of PFTs as these two aspects are not necessarily linked.

In the following sections, we discuss existing upscaling approaches with respect to the use of PFT and LCT information (4.1), the representations of vertical trait variation with TWMs or CWMs (4.2), aspects of the evaluation of the maps (4.3), the potential to use synthesis maps (4.4), the implications for trait ratios, trait-trait and trait-environment relationships (4.5), and ending with an outlook (4.6).

4.1 Upscaling with or without PFTs ?

Both the PFT+Env and the Env upscaling approaches have practical advantages and limitations which partly depend on the characteristics of the *in-situ* data (Table S5). We found that the Env-based maps cannot well capture the between-PFT trait differences (Fig. 5b) and therefore tend to show stronger similarity to key environmental drivers (Figs. 7, 8b, S14b, S15), while they apparently reasonably capture environmentally driven within-PFT variations (Fig. S10). This is directly opposed to the categorical maps that only rely on PFT and LCT information to represent between-PFT differences while, by design, lacking information on within-PFT trait variation (Fig. 8b, Table S5). PFT+Env approaches can combine the two to capture both between- and within-PFT trait variation (Figs. 5b, 6, 8, S10). However, our results show that including PFT and LCT information does not guarantee good performance regarding the representation of between-PFT differences for TWM (Figs. 5a, 6, Table S5). The limitations of Env upscaling approaches to capture between-PFT trait differences is mostly related to the heterogeneity of the majority of the grid cells for which in-situ data is available (Fig. 9a) and better performance would be expected for mostly homogeneous grid cells (Table S5).

Conceptually, the approach used in the PFT+Env upscaling corresponds to a common strategy to account for sub-grid variations by partitioning the heterogeneous patterns into more homogeneous components (Wu, 2007). Consistent with this interpretation, we found that the reduction in within-grid cell trait variability when stratifying by PFT can be considerable, especially for TWMs (Fig. 9b) and is consistent across a wide range of spatial scales (Fig. S17). This reduction in variability is due to the considerable differences in PFT mean trait values which are well documented in the literature (e.g. Reich *et al.*, 2007; Kattge *et al.*, 2011) and also present in sPlotOpen TWM and CWM data (Fig. 5b). While PFT+Env upscaling approaches tend to better capture between-PFT trait differences, some of them are also negatively affected by the heterogeneity of the training data (Table S5) and all of them have limitations regarding the use of LCT cover products to represent canopy cover of the dominant PFTs. The motivations and limitations of global trait upscaling with and without PFT and land cover information are discussed in more detail below (4.1.1 - 4.1.3).

While in the upscaling approaches we analyzed the use of PFT and land cover information is typically associated with the use of TWMs and Env approaches typically aimed at CWMs, these associations are not necessarily always present. Some of the motivations for using PFT and land cover information also apply to CWMs and on the other hand Butler also attempted to upscale TWMs using environmental drivers alone (Figs. 7, 8a, S7, S14) as did Bodegom whose SLA map shows stronger similarities to the Butler Env map for SLA than with the other more CWM-based Env maps (Figs. 6a, 8a). We did not have any upscaled map that combined CWM with PFT and LCT information but can rely on some indications from the analyses made on sPlotOpen data (Figs. 5b, 6, 9) as well as comparisons to TWM in our reasoning.

Conceptually, a fundamental difference between PFT+Env approaches and Env approaches is that the former rely on remotely sensing products such as land cover and surface reflectance to constrain trait values based on observed vegetation characteristics (Fig. 1), while the latter approaches only rely on environmental drivers. This aspect of the upscaling approaches can be related to the distinction of actual or realized versus potential species distributions (Bonannella et al., 2022). Potential distributions are are based on suitable environmental conditions and can be useful for prognostic applications (e.g. Boonman *et al.*, 2022), while realized distributions are based on additional remote sensing observations and more related to monitoring applications. In the upscaling approaches, the more important step for modeling of realized rather than potential trait variation is the spatialization step (Table S5).

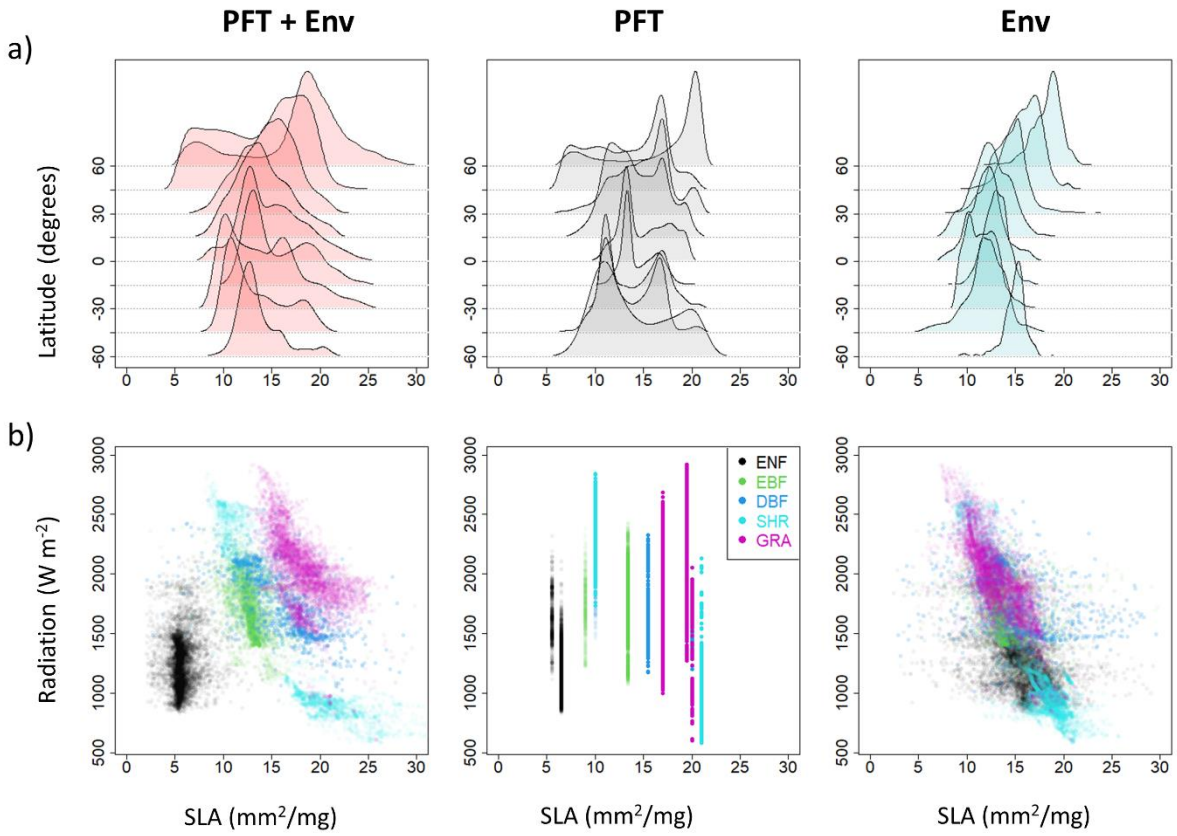

Figure 8: Overview of the impact of different upscaling approaches on latitudinal trait distributions and the corresponding trait-environment relationships. *a) latitudinal distributions of specific leaf area (SLA) for three different upscaling approaches applied to the same in-situ top-of-canopy weighted mean (TWM) data by Butler et al. (2017): the full upscaling model ('PFT+Env') using environmental predictors, plant functional type (PFT) and land cover information, the simplified categorical map ('PFT') only relying on land cover fractions and mean PFT trait values for 14 PFT categories, and the maps only relying on environmental predictors ('Env'). For the sake of direct comparison, the Env spatial model was used here. The latitude values in a) correspond to the minimum value of 15 degree intervals. b) the relationships between solar radiation and the SLA values of the maps shown in a) stratified by land cover type (ENF: evergreen needleleaf forest; EBF: evergreen broadleaf forest; DBF: deciduous broadleaf forest; SHR: shrubland; GRA: grassland). For each land cover type only grid cells with more than 50% cover are shown. For the categorical map ('PFT') in b) each land cover type can have multiple trait values as the 14 PFT categories correspond to the five land cover types with sub-distinctions related to climate zone (e.g. temperate vs. tropical, temperate vs. boreal etc). The maps corresponding to the three columns shown here can be found in Fig. S7a.*

4.1.1 Upscaling with PFTs

Three different perspectives on using PFT and land cover information in upscaling approaches emerge from our study that depend on the starting point or focus. These are addressed in more detail below. In practice, all three perspectives can be compatible with the same type of upscaling algorithm although we found different preferences for certain upscaling approaches depending on the motivation (Fig. 1) and different limitations may be more relevant for one or the other perspective.

(1) **Refining the PFT representation in land surface modeling.** For PFT-based land surface modeling schemes that aim at refining the simplified representation of PFTs as uniform in terms of foliar traits but do not aim to entirely remove PFT categories, the use of PFT and LCT information in the upscaling is an obvious choice. Essentially, the focus is on modeling trait variation within each PFT separately, using this information for e.g. modeling of carbon and water fluxes, and then combining the outputs with LCT cover weighting. It is therefore somewhat surprising that none of the approaches that were motivated by land surface modeling approaches such as Butler and Madani provided upscaled trait outputs separately by PFT. Except for the approach of Moreno, where the upscaling is not done separately for each PFT, the other PFT+Env approaches (Fig. 1, Table 2) are consistent with the land surface modeling framework of PFT-based trait upscaling. It is important to note that in contrast to the simplified PFT-based look-up tables of many land surface models that directly assign a trait value to each PFT, the PFT-based upscaling approaches do not directly constrain trait values with PFT information. Instead, the *in-situ* trait data determine the trait variation within each PFT and only the spatial occurrence of a given PFT is constrained by the land cover (LCT) products. An alternative strategy for better representing within-PFT trait variation without upscaling is to generate trait distributions per PFT (Butler *et al.*, 2022).

(2) **PFT as a useful categorical predictor (spatialization).** As trait-environment relationships can differ between PFTs (e.g. Wright *et al.*, 2005; Fyllas *et al.*, 2020), including PFT information can considerably improve the predictive performance of trait-environment relationships (e.g. Reich *et al.*, 2007; Kambach *et al.*, 2023). Therefore, including PFT information appears attractive to improve upscaling regression models for the spatialization. Conceptually, this use of PFT information could be considered a special case of making use of trait-trait correlations for trait estimation (Reich *et al.*, 2007): a set of categorical traits (growth form, leaf type, leaf phenology) is used to improve the estimation of leaf chemical and morphological traits. If the goal is not only to generate upscaled trait maps per PFT but also have a final trait map that combines all PFTs, the key aspect is to have PFT-related information also in grid cells for which no foliar trait *in-situ* data are available. For this, the LCT maps are crucial and used as proxy for the canopy cover of the dominant PFT. The upscaling approaches of Butler, Madani, and Vallicrosa are consistent with

the motivation of using PFTs as categorical predictors, while the approach of Moreno is not.

(3) **PFTs as tool to account for the lack of representativeness of *in-situ* observations regarding the (horizontal) trait variation within grid cells.** The grid cells of upscaled maps are very large compared to the scale of *in-situ* observations, which were not designed to represent these grid cells but are collections from independent measurement campaigns for very different purposes (Kattge *et al.*, 2011, 2020). More importantly, most of the *in-situ* observations used in the upscaling approaches fall into heterogeneous grid cells regarding land cover (Fig. 9a). Therefore, the *in-situ* data in most grid cells are unlikely representative of the entire grid cell. To account for this lack of representativeness, traits can be averaged first per dominant PFT within each grid cell and then weighted by the contribution from each dominant PFT with the corresponding area fractions from remote sensing based LCT cover products. This aspect of improving the representativeness of *in-situ* observations was most prominent in the Moreno approach, which, in contrast to Butler, Madani and Vallicrosa, only used PFT and LCT information in the leaf-to-grid scaling step (Fig. 1). However, the representativeness aspect is also relevant for the other approaches that used PFT information. Unweighted averaging of *in-situ* trait observations in a grid cell separately for each PFT assumes that the within-PFT trait variation is sufficiently small (Fig. 9b) and does not show strong systematic spatial patterns (Fig. 9c). One important aspect of the motivation to account for the lack of representativeness of *in-situ* data is that, in theory, the performance of the PFT and LCT-based approaches should be relatively independent of the grid cell size. Even for large grid cells, the relevant sub-grid information is contained in the LCT cover fractions. The fact that we found the strongest agreement between the Butler and Moreno maps (Fig. 4) that used 50 km and 1 km grid cell sizes for upscaling, respectively, supports this reasoning.

Limitations

While PFT and LCT information can be very useful for trait upscaling, there are limitations. Most of these limitations are related to the use of LCT products, but some are related more directly to the use of *in-situ* PFT observations.

Limitations of using LCTs. First, by definition, the LCT categories do not directly capture the actual cover fractions of the dominant PFT. For example, based on the IGBP land cover

classification scheme (Loveland & Belward, 1997) used in the widely used MODIS products (Friedl *et al.*, 2002) that applies thresholds, a grid cell with 60% DBF and 40% ENF LCT cover could actually have canopy cover fractions of 40% deciduous broadleaf trees, 30% evergreen needleleaf trees and 30% shrubs, which translates into considerable uncertainties for grid-cell-level foliar trait estimates. The LCT categories are therefore suboptimal for trait estimation based on the dominant PFT. Second, the maps of LCT cover can have considerable uncertainties even when considering only the original land cover class definitions (Congalton *et al.*, 2014). While distinguishing evergreen from deciduous vegetation is rather straightforward with multi-spectral satellite data, finer differences within these categories can be more challenging to capture accurately (e.g., deciduous broadleaf shrubs versus deciduous broadleaf trees). Given these uncertainties and dominance impacts of the land cover information at both the global and more local scales (e.g. Fig. S6, Fig. S7), the differences between the PFT+Env maps could therefore be partly explained by discrepancies between the different land cover products used (Table S2). Third, since the LCT cover is not available for future time periods, or only with even larger uncertainties than the corresponding climate scenarios, using LCTs in upscaling is more suitable for diagnostic purposes, i.e., monitoring, than for predictive purposes. It is important to note, however, that the limitations of LCTs only affect the final step of recombining separately upscaled PFT trait maps in approaches such as Butler and Vallicrosa as the separately upscaled trait maps per PFT did not use LCT information (Fig. 1). Moreno used LCT information in the leaf-to-grid scaling, which therefore also at least partly propagates to the final map even though it was not used in the spatialization step (Fig. 1).

Limitations of using in-situ PFT data. The definition of (dominant) PFTs we used based on growth form, leaf type and leaf phenology, is suboptimal for the purpose of decomposing the entire trait distribution into parts that minimize overlap and well cover the entire trait range (ideally in equidistant intervals without overlap) to reduce within-grid cell trait variability. Another limitation is that some species can change PFT categories depending on the environmental conditions (Wang *et al.*, 2022a), which can make an assignment at the global scale challenging. Both these limitations could be partly addressed/reduced with finer PFT categories by adding climatic information (as done by Butler) as long as sufficient *in-situ* data for each of the finer categories is available. However, some of the original limitations will remain and the use of finer PFT categories might even make the upscaling unnecessary for some applications as we found that the PFT+Env map by Butler can be relatively well approximated by adjusting the mean trait values of the 14 PFT categories used, i.e., generating an optimized categorical map (Fig. S2).

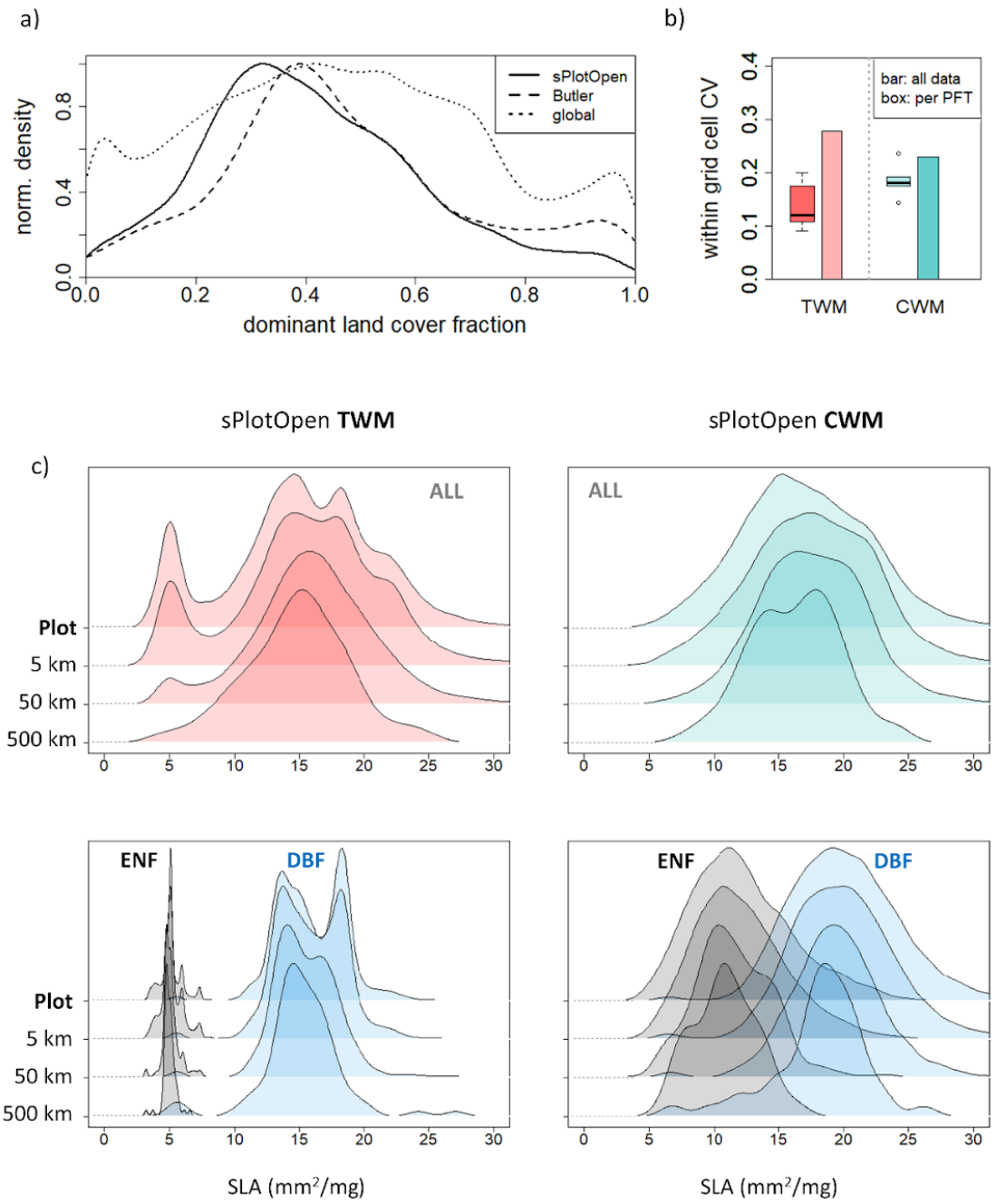

Figure 9: Overview of the impact of different upscaling approaches on latitudinal trait distributions and key aspects related to the heterogeneity of the vegetated land surface. *a) distribution of grid cells regarding the maximum land cover fraction irrespective of the land cover type: sPlotOpen (all plots, N~5000), TRY data selected by Butler et al. (2017)(N~500), or all global vegetated grid cells (N~60000). The maximum fraction represents a measure of land cover homogeneity. b) sPlotOpen global-scale within grid cell (50 km) trait variability as quantified by the coefficient of variation (CV) based on top-of-canopy weighted mean (TWM) or community weighted mean (CWM) data and all available trait data (bar showing median over the global-scale distribution) or stratified per PFT (boxplot summarizing the global medians of the individual plant functional types, i.e., PFTs). c) example of the impacts of unweighted averaging on sPlotOpen TWM and CWM trait distributions in the latitudinal range of 45°-60° north either including all data ('All' in top row) or stratified by PFT for evergreen needleleaf forest (ENF) and deciduous broadleaf forest (DBF). Plot data are shown for reference and three different grid cell sizes with their corresponding size at the equator are given. Note that, conceptually, in c) the top row corresponds to the bars in b), while the bottom row corresponds to the boxplots in b).*

4.1.2 Upscaling without PFTs

There are several reasons to avoid the use of PFT information. First, using discrete and to a certain degree arbitrary PFT categories that show overlapping trait distributions might be unnecessary, if sufficient information is available from *in-situ* data and other suitable predictor variables. Especially if the focus is on upscaling CWMs, relying on PFT information can seem unattractive as differences between dominant PFTs are smaller than for TWMs (Fig. 5b, 9b) and as the objective of CWMs is to use an integrative trait metric. Second, due to the limitations of LCT products (see paragraph above), it would be preferable not to use them to avoid introducing artifacts and additional uncertainties. Third, assuming that the predictors are available for future scenarios with a reasonable level of confidence, which is the case with climate variables, approaches that rely only on climate (and soil) predictors could then be used for estimating future changes in foliar traits, which is relevant for climate change-related applications (e.g. Boonman *et al.*, 2022).

Limitations

Upscaling approaches that do not rely on PFT information face important practical limitations. These limitations affect both the leaf-to-grid and spatialization steps, but the impacts on the leaf-to-grid scaling are considerably more important as information lost in this step cannot be recovered in the spatialization (for those approaches that conducted the spatialization at the end, i.e. excluding Schiller, see Fig. 1). The limitations affect upscaling of TWM more strongly than CWM but are relevant in both cases.

Leaf-to-grid scaling. In the leaf-to-grid scaling, the unweighted averaging over available *in-situ* data effectively assumes either that these data are representative of the grid cells (in the sense that the average over them is close to the average of an ideal, high-resolution trait map) or that there might be biases at smaller scales, but they tend to average out when looking at global scale trait patterns. These assumptions are addressed separately below.

The assumption of representativeness is not well- justified for the following reasons. First, none of the relevant *in-situ* data sources like TRY, sPlotOpen, or citizen science images (Schiller) were sampled in a manner to provide representative trait information for 0.5 degree grid cells. Second, given the trait differences between PFTs Fig. 5b) and the fact that a large fraction of the global vegetated land surface is heterogeneous regarding LCT cover even at 0.5° (Fig. 9a), the representativeness does not emerge simply from large numbers of samples if they are not designed specifically with this goal. Third, TRY and sPlotOpen data, which was used in almost all upscaling approaches (Fig. 1), is mostly located in heterogeneous grid cells

regarding land cover (Fig. 9a), i.e. the situation is even worse than a random sample of vegetated grid cells.

The impact of the lack of representativeness of *in-situ* observations is not limited to small spatial scales. While the impacts can differ across the global land surface, they are most conspicuous when looking at the low values of SLA and N for ENF. The original plot-level sPlotOpen TWM (and *in-situ* TRY) data show a distinct double-peak distribution for SLA in the higher northern latitudes, the peak feature with lower SLA values associated with ENF is either strongly reduced or almost disappears when applying unweighted averaging the *in-situ* data within grid cells (Fig. 9c, Fig. S13). Due to the loss of information already for the reference or training grid cells, the lower trait signal of ENF cannot be well modeled in the spatialization. This results in the absence of a distinct signature of lower SLA and N values in the ENF-dominated region of the northern hemisphere of the Env maps compared to other co-occurring PFTs such as SHR and DBF (Figs. 4, 5). In addition to the findings using sPlotOpen data without spatialization (Figs. 9, S13), the effect of suppression of the low trait values for ENF in upscaled maps without PFT information can be seen in the different versions of the Butler and Moreno upscaled maps based on the same *in-situ* data (Fig. S7, S14a). Interestingly, the use of the spatial information on the locations of *in-situ* data in the prediction can partly overcome this effect in regions with high *in-situ* data density but not elsewhere (Figs. S7a, S14a,b)

The limitations regarding unweighted leaf-to-grid scaling does not only apply to upscaling approaches that applied the leaf-to-grid scaling as first step (Boonman, Bodegom) but also to approaches that first spatialize and then scale a considerably larger number of observations or trait estimates to the grid cells as final step (Schiller) (Fig. 1). The reason for this is that a larger number of grid cells (e.g. one order of magnitude difference Fig. 9a) without targeted sampling towards more homogeneous grid cells does not noticeably change the level of heterogeneity (Fig. 9a). The approach by Wolf et al. (2022) is conceptually similar to the Schiller approach to which it is also most strongly correlated (results not shown) and consequently would fall into the group of Env maps although it did not actually use environmental predictor variables.

Spatialization. In principle, not using PFT or LCT information in the spatialization implies using universal trait-environment relationships across all vegetation types (Figs. 8b, S15). However, trait-environment relationships can show considerable differences between vegetation types (e.g. Reich *et al.*, 2007; Kambach *et al.*, 2023) implying limitations in using universal relationships for upscaling. Among other things, only using environmental predictors

likely increases the uncertainties related with spatialization in regions where the regression models effectively extrapolate (Meyer & Pebesma, 2021). Consistent with this interpretation and in contrast to the PFT+Env maps, the differences between Env maps (Fig. 4) seems to be at least partly related to *in-situ* data availability (Fig. S1). Also, it is noteworthy that the Env maps that partly captured somewhat lower values for ENF only did so in smaller parts of the ENF-dominated regions (e.g. Boonman for N, Fig. S5) such as Europe that has a relatively high density of *in-situ* observations (Fig. S1). The failure to also capture the low ENF trait values in North America and Siberia therefore appears to be related to extrapolation in the environmental predictor space (Boonman *et al.*, 2020) in addition to the aggregation effects due to heterogeneous grid cells in the leaf-to-grid scaling (Figs. 9c, S13).

4.1.3 Limitations affecting both approaches with and without PFT information

While the different limitations appear to clearly separate the approaches with and without PFTs at first sight, there actually is some overlap between them due to the characteristics of the underlying *in-situ* data. The key limitation of *in-situ* data is that it is mostly located in heterogeneous grid cells regarding land cover (Fig. 9a). This implies that even when weighted averages using LCT cover fractions are used in the leaf to grid scaling step, the result is a combination of trait values from different LCTs, which has a rather similar impact on latitudinal trait distributions as unweighted averages, i.e. making the distributions narrower and more unimodal (Fig.S18a). Based on this, even PFT+Env approaches such as the version by Moreno that only used PFT+LCT information in the leaf-to-grid scaling and Env in the spatialization (Fig. S7a, S14a,c) tend to effectively generate trait estimates that better represent heterogeneous grid cells (note that its ability to still partly capture the low values of SLA in ENF dominated regions could also be related to the use of 1 km instead of 50 km grid cells). This results in considerable discrepancies between upscaled maps and the plot-level *in-situ* data for more homogeneous grid cells, which account for an important part of the global vegetated land surface despite the dominance of heterogeneous grid cells (Fig. 9a). While the final model by Moreno used remotely sensed surface reflectance time series, which have a similar information content as the LCT cover products, in the spatialization, this model could apparently not fully recover the trait values of homogeneous grid cells (Figs. 5b, 6, S10a).

Nevertheless, the impact of the mostly heterogeneous training data differs between the Env approaches and the Moreno PFT+ Env approach. While the Moreno SLA and N maps partly show more similarities to the absolute values and latitudinal trait distributions of the Env maps (Fig. 6), the relative spatial patterns of the Moreno map are more similar to the other PFT+Env maps that used LCT information in the spatialization step (Figs. 3, 4). This all suggests that the Moreno approach is intermediate between the Env approaches and the PFT+Env

approaches that separately upscaled per PFT (Butler, Vallicrosa, Madani) (Table S4). These latter approaches can, in principle, better represent trait variation in homogeneous grid cells despite relying on heterogeneous training data as they effectively model *potential* homogeneous grid cells separately per PFT and only re-generate heterogeneous grid cells via the LCT cover weighting in the final step after the spatialization (Fig. 1).

Both the PFT+Env and the Env approaches apparently face challenges to capture the trait values of deciduous needleleaf forest (DNF). Although we excluded DNF from most of our analyses due to the limited data availability, the discrepancies between sPlotOpen and upscaled maps tended to be larger for DNF than for other PFTs when applying the unmixing approach (results not shown) and larger differences between maps of the same category can also be seen in the DNF-dominated region (Fig. 4, S5). While the limitations affect both the PFT+Env and the Env upscaling approaches, the limitations are due to different aspects related to the shortage of *in-situ* data. The PFT+Env approaches that separately upscaled per PFT such as Butler, Madani and Vallicrosa simply lack enough *in-situ* data to well constrain DNF-specific models. The Env approaches face the challenge that available *in-situ* data in locations not dominated by DNF are not representative of the environment where DNF is dominant (Boonman *et al.*, 2020). Recent advances in optimality theory-based trait modeling could help to better constrain the trait values of SLA and N for DNF-dominated regions despite the current lack of *in-situ* observations (Dong et al., 2023, in press).

4.2 Vertical variation of traits within the canopy: upscaling CWMs or TWMs ?

Apart from the horizontal scaling aspects related to the use of PFTs and land cover, the differences in the upscaling approaches regarding the way vertical trait variation was accounted for (CWMs versus TWMs) is an important aspect to consider. While the use of CWMs versus TWMs has considerably smaller impacts on spatial trait patterns than upscaling with PFTs and LCTs or not (Figs. 7c,S18), it is an important additional factor resulting in differences between maps. Using CWMs tends to result in narrower and more unimodal trait distributions with smaller differences between PFTs than for TWMs (Figs. 5b, 6, S9). However, the differences between TWM and CWM depends on the trait. Among foliar traits, we found larger differences for SLA than for N and P (Fig.S18b), which is consistent with the known sensitivity of SLA to light availability (Evans & Poorter, 2001) and other evidence on vertical variation (Ellsworth & Reich, 1993; Davrinche *et al.*, 2023).

While none of the upscaling approaches used CWM or TWM in the same way as done in sPlotOpen, there are nevertheless tendencies towards one or the other. Boonman used an

unweighted community mean at the site level and the approach used by Schiller seems to integrate vertical trait variation to some degree via the information in the citizen science images and therefore tend more towards CWM. The other five approaches tend more towards TWM as they did not explicitly include vertical trait variation and the *in-situ* trait data in the TRY database tends to be collected from sunlit leaves in the top of the canopy. It is noteworthy that while the Bodegom map falls into the Env group, its trait metric at the site level is more similar to TWM, which can explain the considerable similarity in its latitudinal distributions (Fig. 6) compared to the Butler Env map (Fig. 8a). A more detailed discussion on the motivations and limitations of CWMs and TWMs follows below.

4.2.1 CWMs

CWMs are the standard metric for many ecological analyses based on community trait data including trait-trait and trait-environment relationships (Bruelheide *et al.*, 2018; Anderegg, 2022; Guerin *et al.*, 2022), and are routinely applied in the sPlot and sPlotOpen datasets (Bruelheide *et al.*, 2019; Sabatini *et al.*, 2021). The concept of CWMs was introduced in relation to the biomass ratio hypothesis, which states that species contribute to ecosystem characteristics based on their biomass ratio (Garnier *et al.*, 2004), as should their traits. The weighting of traits is commonly done by the basal area, biomass, or leaf area (Anderegg, 2022) or by fractional cover (Sabatini *et al.*, 2021). The goal of CWMs is to integrate all trait variation present in a plant community in a single value that is expected to show more consistent trait-environment relationships than sub-selections of the community (Anderegg, 2022). Applications of CWMs include, among other things, studies of community assembly via environmental sorting or historical biogeographic processes, deciphering the role of traits in ecosystem functioning, or modeling ecosystem properties using a range of approaches.

4.2.2 TWMs

Upscaling top-of-canopy-weighted means (TWMs) can have several different motivations related to land surface modeling, alternatives to the common cover/abundance-based weighting in CWMs, and remote sensing. From the perspective of land surface modeling, the higher levels of a canopy tend to dominate many processes of vegetation-atmosphere interactions such as photosynthesis due to the dominance of leaf area and light availability of top-of-canopy vegetation. Therefore, the trait values of sunlit leaves of dominant PFTs have been widely used in land surface models (Yang *et al.*, 2015). Impacts of reduced light availability that can capture part of the trait variation in lower levels of a canopy are commonly modeled in land surface models (Hikosaka *et al.*, 2016), therefore, the combination of such models with TWM trait values can be useful.

Even when ultimately aiming at CWMs, TWMs can be a relevant practical tool to approximate other weighting strategies when only relative cover fractions are available. The reason is that due to the lack of sufficient data on leaf area or leaf biomass in many datasets, CWMs are frequently calculated using fractional cover or abundance data, which is also the case in sPlotOpen (Sabatini *et al.*, 2021). This, however, implies giving similar weight to understory vegetation as overstory trees as long as their cover fractions are comparable despite large differences in leaf area and leaf biomass. Therefore, when applying a weighting based on leaf area or leaf biomass, a CWM would likely tend more towards TWM than to a cover/abundance-weighting CWM in most situations. Since the data necessary for a leaf area- or leaf biomass-based weighting are not readily available, however, TWMs could be considered a pragmatic approximation to CWMs based on weighting with leaf area/biomass.

From a practical remote sensing perspective, the widely used multi- and hyperspectral sensors used on airplanes and satellites are most sensitive to the top of the canopy. Therefore, if the goal is to compare upscaled maps with remote sensing-based maps, TWMs are a suitable metric. This applies to future global foliar trait maps based on hyperspectral satellite data (see section 4.6) and can also be illustrated with canopy height for which there are already global maps derived from satellite-based lidar instruments (Simard *et al.*, 2011; Wang *et al.*, 2016; Potapov *et al.*, 2021; Lang *et al.*, 2022). While canopy height is admittedly an extreme case due its large differences between CWM and TWM, it can serve as an intuitive example to illustrate the differences in these two metrics: clearly, TWM canopy height is expected to be much larger than CWM canopy height that includes understory vegetation. Unsurprisingly, upscaled canopy height maps based on TWM show a considerably higher level of similarity to satellite-based height maps using lidar information than CWM upscaled maps (Fig. S16). Importantly, the TWM and CWM upscaled maps differ not only considerably regarding their absolute values but also show large differences in their spatial patterns (Fig. S16). While the TWM maps used PFT and land cover information and the CWM maps did not, for canopy height the use of the PFT and land cover information is considerably smaller than the choice of TWM versus CWM, in contrast to the foliar traits (Fig.S18b).

4.3 Evaluation of maps

While the comparison of different upscaling approaches and maps can give important insights into the factors explaining the differences, a higher level of consistency - as observed in the maps using PFT information (Fig. 3) - does not necessarily imply better performance. Therefore, it is important to take other criteria into account. We discuss Internal performance assessments and the evaluation compared to sPlotOpen data products.

4.3.1 Internal performance metrics.

Most of the upscaling approaches provided cross-validation metrics, but their interpretation is complex. Overall, there was a clear pattern of considerably higher R^2 for PFT+Env approaches compared to Env approaches (R2 about 0.6 or higher compared to 0.4 or lower), with larger differences for N compared to SLA. However, these findings can be misleading as the input *in-situ* trait observations differ considerably in terms of the number and the data sources (Fig. 1) and there are limitations of random cross-validation approaches to evaluate mapping performance (Ploton *et al.*, 2020; Meyer & Pebesma, 2021).

Some of the upscaling products also provided estimates of the uncertainty of the mean (standard error) trait values per grid cell. However, these estimates differ considerably in terms of methodology and should be interpreted with caution. In some cases, a single algorithm provided uncertainty estimates (e.g. Bodegom, Vallicrosa), while in one case the differences between different algorithms was used (Boonman). Overall, we found no indications that the uncertainty or variability estimates corresponded to the observed discrepancies between maps, even within the PFT+Env and the Env groups (Figs. 4, S19). An exception to this seems to be the apparent correspondence of the higher CV values for SLA in the Madani product with the higher values of the between-map CV of the PFT+Env maps (Fig. 4). This region of higher discrepancy values is dominated by DNF (Fig. 4 dominant LCT cover) for which trait values cannot be well constrained in the PFT-based upscaling approaches due to the sparsity of *in-situ* observations.

4.3.2 External reference data (sPlotOpen)

Despite its limitations, we think that sPlotOpen is currently the best available open access dataset for evaluating the upscaled maps given its global coverage and the fact that it is based on a characterization of entire plant communities in contrast to individual species. However, as the upscaling approaches differ in the way horizontal (within-grid-cell) and vertical (within canopy) trait variation was taken into account, there is no way to process sPlotOpen data such that it could be used as universal benchmark data for all upscaling approaches. Rather, sPlotOpen can be used as a basis for evaluating the differences in performance *within* a given upscaling framework/strategy regarding the leaf-to-grid scaling. While the above reasoning applies when aiming at direct comparisons between upscaled maps and sPlotOpen data at *grid-cell-level* (Figs. 7, 14c), the upscaling approach-specific adjustment to sPlotOpen data can be restricted to the choice of plot-level trait metric (CWMs or TWMs) when comparing *plot-level* sPlotOpen data to upscaled maps (Figs. 2a, 6, S11). It is therefore instructive to conduct such a comparison of *plot-level* sPlotOpen data to upscaled maps by using latitudinal distributions which, in contrast to global trait distributions, contain some of the relevant spatial

information. Furthermore, the distribution-based comparisons of plot-level versus grid-level sPlotOpen (and TRY) data can provide insights on the impacts of the leaf- or plot-to-grid-scaling step.

We found that both for unweighted and LCT cover-weighted grid-cell averages, the trait distributions of sPlotOpen differed considerably from those of the original plot-level data with a clear tendency of narrower and more unimodal distributions at the grid-cell-level (Figs. 9c,S18a). This is related to the high level of land cover and trait heterogeneity in the grid cells where sPlotOpen data are available (Fig. 9a,b). These results suggest that caution is warranted when interpreting comparisons of upscaled maps with grid-cell-level sPlotOpen data as the latter can differ strongly from the underlying plot-level data. In fact, the characteristics of sPlotOpen data aggregated to the grid-cell-level with unweighted averages strongly depend on the chosen grid cell size (Figs. 9b, S13), with smaller grid cell sizes showing trait distributions more similar to plot-level data. While there can, of course, be 'real' resolution dependencies of trait distributions, our analyses show that the impacts we observed are primarily due to the unweighted averaging as the PFT component distributions show a considerable level of robustness across grid cell sizes (Fig. 9b). The impact of resolution of unweighted averaging on sPlotOpen data itself is not surprising as e.g. in 1 km grid cells, most grid cells will only contain a single plot (or a small number or more similar ones), which strongly reduces the impacts of averaging. However, this does not mean that these grid cells are in fact homogeneous in terms of land cover (Yu *et al.*, 2018) or trait variation (see versions of Moreno maps without PFT information in Fig. S7 based on 1 km grid cells).

Regarding the evaluation of PFT+Env maps with grid-cell-level sPlotOpen data, our results indicate that a comparison stratified per PFT (Figs. S9, S10) is more meaningful than at the level of the final maps. First, when using the final maps after applying the LCT cover-weighted averages, highly simplified categorical trait maps, which were the motivation for improvement using PFT+Env upscaling, can achieve a similar level of agreement with sPlotOpen reference data (Fig. 7a). Second, the PFT-stratified evaluation directly quantifies the similarities between upscaled maps and sPlotOpen at the level of within-PFT trait variation that was the main motivation of the upscaling (e.g. Butler). Our findings also indicate that the between-PFT trait differences should be evaluated in addition to the within-PFT variations as, in contrast to what might be expected, they can differ considerably even between PFT+Env approaches (Figs. 5b, S10). Therefore, future PFT+Env upscaling approaches should provide the intermediate trait maps upscaled per PFT in addition to the final maps to facilitate intercomparisons and evaluations. While we showed that the final maps can, in principle, be separated into PFT

components (Figs. S2, S3), this approach introduces unnecessary additional uncertainties which can be avoided by using the direct outputs from the upscaling.

One limitation of the sPlotOpen dataset is that it ignores intra-specific trait variations as global-scale species mean trait values from the TRY database were used (Sabatini *et al.*, 2021). While the impact on the global-scale trait pattern of this might be small in most regions due to the dominance of species composition and abundances on CWMs and TWMs, we found that the strong tendency towards higher trait values of the Butler maps at high latitudes was apparently at least partly caused by strong intraspecific variations in the *in-situ* trait data of some species (Fig. S20). Therefore, it remains unclear to what degree the discrepancies between sPlotOpen and the Butler maps in high latitudes for DBF and SHR (Fig. S10) are due to limitations of the Butler maps or sPlotOpen-based trait estimates. In any case, accounting for intra-specific variation in traits in biomes dominated by small numbers of widely distributed species (Bjorkman *et al.*, 2018) will be critical for useful trait parameterization in land surface models (Reich et al. 2014), because populations within widely distributed species often vary markedly in traits due to both genotypic and phenotypic variation, both of which will be further influenced by climate change (Oleksyn *et al.*, 2020).

4.4 Synthesis maps

A relevant question for applications is whether generating synthesis maps per upscaling group (PFT+Env, Env) that outperform the individual maps is feasible and defendable. While the simple average over all maps for a given trait and upscaling category is useful for illustrating some general differences between the two upscaling category (Figs. 4-6), we did not find any evidence that these average maps performed better than the best individual map when evaluated with sPlotOpen (Fig. 7).

For PFT+Env maps, the preferred strategy for generating synthesis maps would be at the level of trait maps per PFT where averaging over different upscaling approaches could be conducted weighted by the agreement to suitable reference data such as sPlotOpen regarding the within-PFT trait variation. However, we could not apply this approach due to the limitations of the separation of upscaled maps into their underlying PFT components (Fig. 2).

4.5 Trait ratios, trait-trait, and trait-environment relationships

While our focus was on the comparison and evaluation of individual foliar traits other aspects of the upscaled maps such as trait ratios, trait-trait and trait-environment relationships are also relevant for ecological applications and could be seen as additional aspects to consider.

Trait ratios. Our focus was on SLA, and N and P concentrations (per mass) as they are key traits that also were among the most commonly upscaled foliar traits. However, trait ratios such as N:P are also of considerable interest as are N and P contents (per area). The foliar chemical contents can also be considered ratios of the corresponding trait (N or P) per mass and leaf mass per area (i.e. 1/SLA) and are therefore included in the reasoning related to trait ratios here. While it is straightforward to calculate trait ratios, such as N:P, from the individually upscaled traits and we found that the ratios appear to be somewhat more consistent between upscaling approaches than the individual traits (results not shown), trait ratios should be directly upscaled for optimal results (Vallicrosa *et al.*, 2022). For N:P this has only been done in relatively few approaches (e.g. Moreno-Martínez *et al.*, 2018; Vallicrosa *et al.*, 2022; Wolf *et al.*, 2022).

Trait-trait correlations. Given the differences in individual trait maps, it is not surprising to also find considerable differences in trait-trait correlations, even within a given upscaling category. We indeed found considerable differences in trait-trait relationships both at the global scale and the local scales using the moving window approach (results not shown). Notably, there were considerable differences between the Butler and Moreno maps regarding the SLA-N relationships, partly differing relatively consistently in the sign of the local correlations (results not shown), despite the relatively high level of correlation for the individual traits (Fig. 3).

Trait-environment relationships. Regarding trait-environment relationships, given the differences between upscaled maps it is to be expected that they also differ as they are an important part of the upscaling methodology. In a sense, comparing trait-environment relationships can be another approach to quantify, illustrate, or understand the differences between the upscaled maps. We did this with the PFT stratified maps and sPlotOpen data, which reveals considerable differences both between the two upscaling categories and within them (Figs. 8b, S15). Note that for PFT-based maps, it is crucial to either select homogeneous grid cells (regarding trait variability, not only land cover homogeneity) or the separately upscaled (or unmixed) maps per PFT/LCT for such analyses as otherwise the land cover information strongly distorts the trait-environment relationships (results not shown).

4.6 Future opportunities

Future upscaling efforts will benefit from progress in areas relevant for foliar trait upscaling related to both the leaf-to-grid and spatialization steps (Fig. 1). *In-situ* trait databases such as

TRY have already been increasing in the volume of available data (Kattge *et al.*, 2020) and the combination of different trait databases can further maximize the available data as shown by Vallicrosa. Furthermore, plot databases such as sPlot are also rapidly growing (https://www.idiv.de/de/sdiv/working-groups/wg-pool/splot/splot-database.html) and can also be used as the basis for upscaling. However, increases in the amount of *in-situ* data do not necessarily lead to increased representativeness for grid cells (Fig. 9a). Regarding the evaluation, sPlotOpen data could be refined to at least partly include intraspecific trait variation for species where sufficient data is available.

To reduce the uncertainties stemming from the leaf-to-grid scaling step in the upscaling, a logical approach is to decrease the size of grid cells to better match the resolution of the *in-situ* observations and increase the fraction of homogeneous reference grid cells. Promising efforts in this respect have made use of high-resolution air- and spaceborne imagery to directly link tree canopies to satellite remote sensing predictors and generate regional or national-scale trait maps (Asner *et al.*, 2016; Aguirre-Gutiérrez *et al.*, 2021), but have not yet been applied at the global scale.

Given the increase in the availability of satellite imagery with both high spatial and temporal resolution (e.g. Houborg & McCabe, 2018), there is potential to improve LCT cover maps to better approximate actual PFT cover fractions. Several improved products have already been generated (Macander *et al.*, 2022; Wang *et al.*, 2022b; Harper *et al.*, 2023). Harper et al. (2022) used high-resolution (30 m) tree cover and canopy height maps to refine global, long-term land cover products in an attempt to better approximate actual PFT canopy cover. Wang et al. (2022) applied a somewhat similar approach using only tree cover to Canada and Alaska. Macander et al. (2022) generated long-term, high resolution (30 m) top cover for seven PFTs across Alaska and parts of Canada. Also, individual tree crowns can now be detected at large scales (e.g. Mugabowindekwe *et al.*, 2022; Wang *et al.*, 2023) and could be further classified into PFTs with time series data or combined with existing high-resolution land cover products in approaches similar to Harper et al. (2022). All these efforts could help reduce uncertainties in upscaled maps that use PFT information.

Different approaches have been developed that try to use stronger predictors of foliar traits than environmental drivers and PFT information. On the one hand, *species occurrence* data from large databases such as GBIF or iNaturalist have been combined with machine learning techniques (Wolf *et al.*, 2022) (Moreno-Martínez et al., in prep.) in an effort to make use of the strong predictive power of species and phylogeny(Kattge *et al.*, 2011; Vallicrosa *et al.*, 2021; Maynard *et al.*, 2022). On the other hand, hyperspectral reflectance of plant canopies in the

visible and near-infrared range has already been successfully used to map foliar traits at regional scales based on airborne remote sensing (Asner & Martin, 2016; Wang *et al.*, 2020). Importantly, these applications demonstrated the ability to capture spatial, intra- and inter-annual temporal (Chlus & Townsend, 2022)(Zheng et al., in prep.) and vertical trait variation (Chlus *et al.*, 2020). Therefore, the hyperspectral-based trait mapping approach has great potential for operational, global-scale foliar trait estimation monitoring (Jetz *et al.*, 2016), especially given that hyperspectral satellite imagery is increasingly becoming available (Zeng *et al.*, 2022).

5. Conclusions and recommendations

We identified two categories of upscaling approaches that result in global, upscaled maps with strongly differing, and partly even opposed spatial patterns. Despite differences in many aspects of the upscaling approaches across these two categories, the use of PFT and land cover information was the dominant factor explaining the differences between the resulting maps. Differences in accounting for vertical trait variation (top-of-canopy versus community mean) were also relevant but had smaller impacts on the spatial patterns of foliar traits than the use of PFT and land cover data. Maps that used PFT and land cover information showed larger trait differences between PFTs and agreed better with sPlotOpen data than the maps only relying on environmental predictor information. Not accounting for within-grid-cell trait variation tends to suppress extremes of the trait distributions, which effectively reduces trait differences between PFTs and leads to more unimodal trait distributions with larger impacts on top-of-canopy trait values. Importantly, these effects also show a strong dependence on grid cell size with stronger impacts at larger grid cell sizes. While the use of PFT and land cover information can partly counteract these effects, the land cover information introduces other uncertainties and has dominant impacts on the global spatial patterns of trait variation.

Based on the insights from our study, we identified four recommendations that are relevant for future upscaling and/or evaluation efforts:

1. Upscaling products should clearly (and prominently) specify the type of trait metric used at the site or plot level (e.g. top-of-canopy versus community; weighted versus unweighted means; type of weighting factor), the type of scaling to the grid cell level (weighted/unweighted, type of weighting factor) and the type of predictor information used (i.e. environmental drivers, remote sensing data, land cover products etc.).

2. In the evaluation of maps with reference data such as sPlotOpen at grid cell sizes much coarser than the *in-situ* plots, comparable scaling as for the upscaled maps should be applied (for grid-cell-level evaluation). Furthermore, comparisons of the distributions of *plot*-level reference data with those of upscaled maps can provide valuable additional insights. For maps using PFT and land cover information, an evaluation at the level of separately upscaled maps per PFT is recommended to directly quantify the agreement of between- and within-PFT trait variation independently of the impacts of land cover that dominate the final maps per trait.
3. Future upscaling efforts should aim at reducing uncertainties by better matching the scale of *in-situ* observations with high-resolution predictor data and ideally also by using predictors with a stronger link to foliar traits than environmental variables.
4. Future trait sampling efforts should consider the aspect of homogeneous grid cells in terms of land cover as well as representativeness at the global scale regarding geographic aspects and covering the full range of key environmental drivers.

Acknowledgements

This paper is a joint effort of the working group sTRAITS kindly supported by sDiv, the Synthesis Centre of the German Centre for Integrative Biodiversity Research (iDiv) Halle-Jena-Leipzig, funded by the German Research Foundation (FZT 118, 02548816). A portion of this research was carried out at the Jet Propulsion Laboratory, California Institute of Technology, under a contract with the National Aeronautics and Space Administration (80NM0018D0004) and through the NSF Biology Integration Institute ASCEND (DBI: 2021898). This research was also supported by the European Research Council under the ERC-SyG-2019 USMILE project (grant agreement 855187). J.A.-G. was funded by the Natural Environment Research Council (NERC; NE/T011084/1) and the Oxford University Jhon Fell Fund (10667). I.H.M.-S. was funded by the NERC grants ShrubTundra (NE/M016323/1) and Tundra Time (NE/W006448/1).

References

Aguirre-Gutiérrez, J., Rifai, S., Shenkin, A., Oliveras, I., Bentley, L.P., Svátek, M., Girardin, C.A.J., Both, S., Riutta, T., Berenguer, E., Kissling, W.D., Bauman, D., Raab, N., Moore, S., Farfan-Rios, W., Figueiredo, A.E.S., Reis, S.M., Ndong, J.E., Ondo, F.E., N'ssi Bengone, N., Mihindou, V., Moraes de Seixas, M.M., Adu-Bredu, S., Abernethy, K., Asner, G.P., Barlow, J., Burslem, D.F.R.P., Coomes, D.A., Cernusak, L.A., Dargie, G.C., Enquist, B.J., Ewers, R.M., Ferreira, J., Jeffery, K.J., Joly, C.A., Lewis, S.L., Marimon-Junior, B.H., Martin, R.E., Morandi, P.S., Phillips, O.L., Quesada, C.A., Salinas, N., Schwantes Marimon, B., Silman, M., Teh, Y.A., White, L.J.T. & Malhi, Y. (2021) Pantropical modelling of canopy functional traits using Sentinel-2 remote sensing data. *Remote Sensing of Environment*, **252**, 112122.

Anderegg, L.D.L. (2022) Why can't we predict traits from the environment? *New Phytologist*, nph.18586.

Asner, G.P., Knapp, D.E., Anderson, C.B., Martin, R.E. & Vaughn, N. (2016) Large-scale climatic and geophysical controls on the leaf economics spectrum. *Proceedings of the National Academy of Sciences*, 201604863.

Asner, G.P. & Martin, R.E. (2016) Spectranomics: Emerging science and conservation opportunities at the interface of biodiversity and remote sensing. *Global Ecology and Conservation*, **8**, 212–219.

Bjorkman, A.D., Myers-Smith, I.H., Elmendorf, S.C., Normand, S., Rüger, N., Beck, P.S., Blach-Overgaard, A., Blok, D., Cornelissen, J.H.C. & Forbes, B.C. (2018) Plant functional trait change across a warming tundra biome. *Nature*, **562**, 57–62.

van Bodegom, P.M., Douma, J.C. & Verheijen, L.M. (2014) A fully traits-based approach to modeling global vegetation distribution. *Proceedings of the National Academy of Sciences*, **111**, 13733–13738.

Bongers, F.J., Schmid, B., Bruelheide, H., Bongers, F., Li, S., von Oheimb, G., Li, Y., Cheng, A., Ma, K. & Liu, X. (2021) Functional diversity effects on productivity increase with age in a forest biodiversity experiment. *Nature Ecology & Evolution*, **5**, 1594–1603.

Boonman, C.C., Huijbregts, M.A., Benítez-López, A., Schipper, A.M., Thuiller, W. & Santini, L. (2022) Trait-based projections of climate change effects on global biome distributions. *Diversity and Distributions*, **28**, 25–37.

Boonman, C.C.F., Benítez-López, A., Schipper, A.M., Thuiller, W., Anand, M., Cerabolini, B.E.L., Cornelissen, J.H.C., Gonzalez-Melo, A., Hattingh, W.N., Higuchi, P., Laughlin, D.C., Onipchenko, V.G., Peñuelas, J., Poorter, L., Soudzilovskaia, N.A., Huijbregts, M.A.J. & Santini, L. (2020) Assessing the reliability of predicted plant trait distributions at the global scale. *Global Ecology and Biogeography*, **29**, 1034–1051.

Bruelheide, H., Dengler, J., Jiménez-Alfaro, B., Purschke, O., Hennekens, S.M., Chytrý, M., Pillar, V.D., Jansen, F., Kattge, J., Sandel, B., Aubin, I., Biurrun, I., Field, R., Haider, S., Jandt, U., Lenoir, J., Peet, R.K., Peyre, G., Sabatini, F.M., Schmidt, M., Schrodt, F., Winter, M., Aćić, S., Agrillo, E., Alvarez, M., Ambarlı, D., Angelini, P., Apostolova, I., Arfin Khan, M.A.S., Arnst, E., Attorre, F., Baraloto, C., Beckmann, M., Berg, C., Bergeron, Y., Bergmeier, E., Bjorkman, A.D., Bondareva, V., Borchardt, P., Botta-Dukát, Z., Boyle, B., Breen, A., Brisse, H., Byun, C., Cabido, M.R., Casella, L., Cayuela, L., Černý, T., Chepinoga, V., Csiky, J., Curran, M., Ćušterevska, R., Dajić Stevanović, Z., De Bie, E., de Ruffray, P., De Sanctis, M., Dimopoulos, P., Dressler, S., Ejrnæs, R., El-Sheikh, M.A.E.M., Enquist, B., Ewald, J., Fagúndez, J., Finckh, M., Font, X., Forey, E., Fotiadis, G., García-Mijangos, I., Gasper, A.L., Golub, V., Gutierrez, A.G., Hatim, M.Z., He, T., Higuchi, P., Holubová, D., Hölzel, N., Homeier, J., Indreica, A., Işık Gürsoy, D., Jansen, S., Janssen, J., Jedrzejek, B., Jiroušek, M., Jürgens, N., Kącki, Z., Kavgacı, A., Kearsley, E., Kessler, M., Knollová, I., Kolomiychuk, V., Korolyuk, A., Kozhevnikova, M., Kozub, Ł., Krstonošić, D., Kühl, H., Kühn, I., Kuzemko, A., Küzmič, F., Landucci, F., Lee, M.T., Levesley, A., Li, C., Liu, H., Lopez-Gonzalez, G., Lysenko, T., Macanović, A., Mahdavi, P., Manning, P., Marcenò, C., Martynenko, V., Mencuccini, M., Minden, V., Moeslund, J.E., Moretti, M., Müller, J.V., Munzinger, J., Niinemets, Ü., Nobis, M., Noroozi, J., Nowak, A., Onyshchenko, V., Overbeck, G.E., Ozinga, W.A., Pauchard, A., Pedashenko, H., Peñuelas, J., Pérez-Haase, A., Peterka, T., Petřík, P., Phillips, O.L., Prokhorov, V., Rašomavičius, V., Revermann, R., Rodwell, J., Ruprecht, E., Rūsiņa, S., Samimi, C., Schaminée, J.H.J., Schmiedel, U., Šibík, J., Šilc, U., Škvorc, Ž., Smyth, A., Sop, T., Sopotlieva, D., Sparrow, B., Stančić, Z., Svenning, J., Swacha, G., Tang, Z., Tsiripidis, I., Turtureanu, P.D., Uğurlu, E., Uogintas, D., Valachovič, M., Vanselow, K.A., Vashenyak, Y., Vassilev, K., Vélez-Martin, E., Venanzoni, R., Vibrans, A.C., Violle, C., Virtanen, R., Wehrden, H., Wagner, V., Walker, D.A., Wana, D., Weiher, E., Wesche, K., Whitfeld, T., Willner, W., Wiser, S., Wohlgemuth, T., Yamalov, S., Zizka, G. &

Zverev, A. (2019) sPlot – A new tool for global vegetation analyses. *Journal of Vegetation Science*, **30**, 161–186.

Bruelheide, H., Dengler, J., Purschke, O., Lenoir, J., Jiménez-Alfaro, B., Hennekens, S.M., Botta-Dukát, Z., Chytrý, M., Field, R., Jansen, F., Kattge, J., Pillar, V.D., Schrodt, F., Mahecha, M.D., Peet, R.K., Sandel, B., van Bodegom, P., Altman, J., Alvarez-Dávila, E., Arfin Khan, M.A.S., Attorre, F., Aubin, I., Baraloto, C., Barroso, J.G., Bauters, M., Bergmeier, E., Biurrun, I., Bjorkman, A.D., Blonder, B., Čarni, A., Cayuela, L., Černý, T., Cornelissen, J.H.C., Craven, D., Dainese, M., Derroire, G., De Sanctis, M., Díaz, S., Doležal, J., Farfan-Rios, W., Feldpausch, T.R., Fenton, N.J., Garnier, E., Guerin, G.R., Gutiérrez, A.G., Haider, S., Hattab, T., Henry, G., Hérault, B., Higuchi, P., Hölzel, N., Homeier, J., Jentsch, A., Jürgens, N., Kącki, Z., Karger, D.N., Kessler, M., Kleyer, M., Knollová, I., Korolyuk, A.Y., Kühn, I., Laughlin, D.C., Lens, F., Loos, J., Louault, F., Lyubenova, M.I., Malhi, Y., Marcenò, C., Mencuccini, M., Müller, J.V., Munzinger, J., Myers-Smith, I.H., Neill, D.A., Niinemets, Ü., Orwin, K.H., Ozinga, W.A., Penuelas, J., Pérez-Haase, A., Petřík, P., Phillips, O.L., Pärtel, M., Reich, P.B., Römermann, C., Rodrigues, A.V., Sabatini, F.M., Sardans, J., Schmidt, M., Seidler, G., Silva Espejo, J.E., Silveira, M., Smyth, A., Sporbert, M., Svenning, J.-C., Tang, Z., Thomas, R., Tsiripidis, I., Vassilev, K., Violle, C., Virtanen, R., Weiher, E., Welk, E., Wesche, K., Winter, M., Wirth, C. & Jandt, U. (2018) Global trait–environment relationships of plant communities. *Nature Ecology & Evolution*, **2**, 1906–1917.

Butler, E.E., Datta, A., Flores-Moreno, H., Chen, M., Wythers, K.R., Fazayeli, F., Banerjee, A., Atkin, O.K., Kattge, J., Amiaud, B., Blonder, B., Boenisch, G., Bond-Lamberty, B., Brown, K.A., Byun, C., Campetella, G., Cerabolini, B.E.L., Cornelissen, J.H.C., Craine, J.M., Craven, D., de Vries, F.T., Díaz, S., Domingues, T.F., Forey, E., González-Melo, A., Gross, N., Han, W., Hattingh, W.N., Hickler, T., Jansen, S., Kramer, K., Kraft, N.J.B., Kurokawa, H., Laughlin, D.C., Meir, P., Minden, V., Niinemets, Ü., Onoda, Y., Peñuelas, J., Read, Q., Sack, L., Schamp, B., Soudzilovskaia, N.A., Spasojevic, M.J., Sosinski, E., Thornton, P.E., Valladares, F., van Bodegom, P.M., Williams, M., Wirth, C. & Reich, P.B. (2017) Mapping local and global variability in plant trait distributions. *Proceedings of the National Academy of Sciences*, **114**, E10937–E10946.

Butler, E.E., Wythers, K.R., Flores-Moreno, H., Ricciuto, D.M., Datta, A., Banerjee, A., Atkin, O.K., Kattge, J., Thornton, P.E., Anand, M., Burrascano, S., Byun, C., Cornelissen, J.H.C., Forey, E., Jansen, S., Kramer, K., Minden, V. & Reich, P.B. (2022) Increasing Functional Diversity in a Global Land Surface Model Illustrates Uncertainties Related to Parameter Simplification. *Journal of Geophysical Research: Biogeosciences*, **127**.

Chlus, A., Kruger, E.L. & Townsend, P.A. (2020) Mapping three-dimensional variation in leaf mass per area with imaging spectroscopy and lidar in a temperate broadleaf forest. *Remote Sensing of Environment*, 12.

Chlus, A. & Townsend, P.A. (2022) Characterizing seasonal variation in foliar biochemistry with airborne imaging spectroscopy. *Remote Sensing of Environment*, **275**, 113023.

Congalton, R.G., Gu, J., Yadav, K., Thenkabail, P. & Ozdogan, M. (2014) Global land cover mapping: A review and uncertainty analysis. *Remote Sensing*, **6**, 12070–12093.

Davrinche, A., Bittner, A., Bruelheide, H., Albert, G., Harpole, S. & Haider, S. (2023) *High within-tree leaf trait variation and its response to species diversity and soil nutrients*, Ecology.

Díaz, S., Kattge, J., Cornelissen, J.H.C., Wright, I.J., Lavorel, S., Dray, S., Reu, B., Kleyer, M., Wirth, C., Colin Prentice, I., Garnier, E., Bönisch, G., Westoby, M., Poorter, H., Reich, P.B., Moles, A.T., Dickie, J., Gillison, A.N., Zanne, A.E., Chave, J., Joseph Wright, S., Sheremet'ev, S.N., Jactel, H., Baraloto, C., Cerabolini, B., Pierce, S., Shipley, B., Kirkup, D., Casanoves, F., Joswig, J.S., Günther, A., Falczuk, V., Rüger, N., Mahecha, M.D. & Gorné, L.D. (2015) The global spectrum of plant form and function. *Nature*, **529**, 167–171.

Ellsworth, D.S. & Reich, P.B. (1993) Canopy structure and vertical patterns of photosynthesis and related leaf traits in a deciduous forest. *Oecologia*, **96**, 169–178.

Evans, J. & Poorter, H. (2001) Photosynthetic acclimation of plants to growth irradiance: the relative importance of specific leaf area and nitrogen partitioning in maximizing carbon gain. *Plant, Cell & Environment*, **24**, 755–767.

Friedl, M.A., McIver, D.K., Hodges, J.C.F., Zhang, X.Y., Muchoney, D., Strahler, A.H., Woodcock, C.E., Gopal, S., Schneider, A., Cooper, A., Baccini, A., Gao, F. & Schaaf, C. (2002) Global land cover mapping from MODIS: algorithms and early results. *Remote Sensing of Environment*, **83**, 287–302.

Fyllas, N.M., Michelaki, C., Galanidis, A., Evangelou, E., Zaragoza-Castells, J., Dimitrakopoulos, P.G., Tsadilas, C., Arianoutsou, M. & Lloyd, J. (2020) Functional Trait Variation Among and Within Species and Plant Functional Types in Mountainous Mediterranean Forests. *Frontiers in Plant Science*, **11**, 212.

Garnier, E., Cortez, J., Billès, G., Navas, M.-L., Roumet, C., Debussche, M., Laurent, G., Blanchard, A., Aubry, D., Bellmann, A., Neill, C. & Toussaint, J.-P. (2004) PLANT FUNCTIONAL MARKERS CAPTURE ECOSYSTEM PROPERTIES DURING SECONDARY SUCCESSION. *Ecology*, **85**, 2630–2637.

Guerin, G.R., Gallagher, R.V., Wright, I.J., Andrew, S.C., Falster, D.S., Wenk, E., Munroe, S.E.M., Lowe, A.J. & Sparrow, B. (2022) Environmental associations of abundance-weighted functional traits in Australian plant communities. *Basic and Applied Ecology*, **58**, 98–109.

Harper, K.L., Lamarche, C., Hartley, A., Peylin, P., Ottlé, C., Bastrikov, V., San Martín, R., Bohnenstengel, S.I., Kirches, G., Boettcher, M., Shevchuk, R., Brockmann, C. & Defourny, P. (2023) A 29-year time series of annual 300 m resolution plant-functional-type maps for climate models. *Earth System Science Data*, **15**, 1465–1499.

Hijmans, R.J. (2022) raster: Geographic Data Analysis and Modeling. R package version 3.5-15. *R package*.

Hijmans, R.J., Van Etten, J., Cheng, J., Mattiuzzi, M., Sumner, M., Greenberg, J.A., Lamigueiro, O.P., Bevan, A., Racine, E.B. & Shortridge, A. (2015) Package 'raster.' *R package*.

Hikosaka, K., Kumagai, T. & Ito, A. (2016) Modeling canopy photosynthesis. *Canopy photosynthesis: from basics to applications*, 239–268.

Houborg, R. & McCabe, M.F. (2018) A Cubesat enabled Spatio-Temporal Enhancement Method (CESTEM) utilizing Planet, Landsat and MODIS data. *Remote Sensing of Environment*, **209**, 211–226.

Jetz, W., Cavender-Bares, J., Pavlick, R., Schimel, D., Davis, F.W., Asner, G.P., Guralnick, R., Kattge, J., Latimer, A.M., Moorcroft, P., Schaepman, M.E., Schildhauer, M.P., Schneider, F.D., Schrodt, F., Stahl, U. & Ustin, S.L. (2016) Monitoring plant functional diversity from space. *Nature Plants*, **2**, 16024.

Kambach, S., Sabatini, F.M., Attorre, F., Biurrun, I., Boenisch, G., Bonari, G., Čarni, A., Carranza, M.L., Chiarucci, A., Chytrý, M., Dengler, J., Garbolino, E., Golub, V., Güler, B., Jandt, U., Jansen, J., Jašková, A., Jiménez-Alfaro, B., Karger, D.N., Kattge, J., Knollová, I., Midolo, G., Moeslund, J.E., Pielech, R., Rašomavičius, V., Rūsiņa, S., Šibík, J., Stančić, Z., Stanisci, A., Svenning, J.-C., Yamalov, S., Zimmermann, N.E. & Bruelheide, H. (2023) Climate-trait relationships exhibit strong habitat specificity in plant communities across Europe. *Nature Communications*, **14**, 712.

Kattge, J., Bönisch, G., Díaz, S., Lavorel, S., Prentice, I.C., Leadley, P., Tautenhahn, S., Werner, G.D., Aakala, T. & Abedi, M. (2020) TRY plant trait database–enhanced coverage and open access. *Global change biology*, **26**, 119–188.

Kattge, J., DíAz, S., Lavorel, S., Prentice, I.C., Leadley, P., BöNisch, G., Garnier, E., Westoby, M., Reich, P.B., Wright, I.J., Cornelissen, J.H.C., Violle, C., Harrison, S.P., Van BODEGOM, P.M., Reichstein, M., Enquist, B.J., Soudzilovskaia, N.A., Ackerly, D.D., Anand, M., Atkin, O., Bahn, M., Baker, T.R., Baldocchi, D., Bekker, R., Blanco, C.C., Blonder, B., Bond, W.J., Bradstock, R., Bunker, D.E., Casanoves, F., Cavender-Bares, J., Chambers, J.Q., Chapin Iii, F.S., Chave, J., Coomes, D., Cornwell, W.K., Craine, J.M., Dobrin, B.H., Duarte, L., Durka, W., Elser, J., Esser, G., Estiarte, M., Fagan, W.F., Fang, J., FernáNdez-MéNdez, F., Fidelis, A., Finegan, B., Flores, O., Ford, H., Frank,

D., Freschet, G.T., Fyllas, N.M., Gallagher, R.V., Green, W.A., Gutierrez, A.G., Hickler, T., Higgins, S.I., Hodgson, J.G., Jalili, A., Jansen, S., Joly, C.A., Kerkhoff, A.J., Kirkup, D., Kitajima, K., Kleyer, M., Klotz, S., Knops, J.M.H., Kramer, K., KüHn, I., Kurokawa, H., Laughlin, D., Lee, T.D., Leishman, M., Lens, F., Lenz, T., Lewis, S.L., Lloyd, J., Llusià, J., Louault, F., Ma, S., Mahecha, M.D., Manning, P., Massad, T., Medlyn, B.E., Messier, J., Moles, A.T., MüLler, S.C., Nadrowski, K., Naeem, S., Niinemets, ü., NöLlert, S., NüSke, A., Ogaya, R., Oleksyn, J., Onipchenko, V.G., Onoda, Y., OrdoñEz, J., Overbeck, G., Ozinga, W.A., PatiñO, S., Paula, S., Pausas, J.G., PeñUelas, J., Phillips, O.L., Pillar, V., Poorter, H., Poorter, L., Poschlod, P., Prinzing, A., Proulx, R., Rammig, A., Reinsch, S., Reu, B., Sack, L., Salgado-Negret, B., Sardans, J., Shiodera, S., Shipley, B., Siefert, A., Sosinski, E., Soussana, J.-F., Swaine, E., Swenson, N., Thompson, K., Thornton, P., Waldram, M., Weiher, E., White, M., White, S., Wright, S.J., Yguel, B., Zaehle, S., Zanne, A.E. & Wirth, C. (2011) TRY - a global database of plant traits. *Global Change Biology*, **17**, 2905–2935.

Kattge, J., Knorr, W., Raddatz, T. & Wirth, C. (2009) Quantifying photosynthetic capacity and its relationship to leaf nitrogen content for global-scale terrestrial biosphere models. *Global Change Biology*, **15**, 976–991.

Lang, N., Kalischek, N., Armston, J., Schindler, K., Dubayah, R. & Wegner, J.D. (2022) Global canopy height regression and uncertainty estimation from GEDI LIDAR waveforms with deep ensembles. *Remote Sensing of Environment*, **268**, 112760.

Lawrence, P.J. & Chase, T.N. (2007) Representing a new MODIS consistent land surface in the Community Land Model (CLM 3.0). *Journal of Geophysical Research*, **112**, G01023.

Loozen, Y., Rebel, K.T., de Jong, S.M., Lu, M., Ollinger, S.V., Wassen, M.J. & Karssenberg, D. (2020) Mapping canopy nitrogen in European forests using remote sensing and environmental variables with the random forests method. *Remote Sensing of Environment*, **247**, 111933.

Loveland, T.R. & Belward, A.S. (1997) The IGBP-DIS global 1km land cover data set, DISCover: First results. *International Journal of Remote Sensing*, **18**, 3289–3295.

Macander, M.J., Nelson, P.R., Nawrocki, T.W., Frost, G.V., Orndahl, K.M., Palm, E.C., Wells, A.F. & Goetz, S.J. (2022) Time-series maps reveal widespread change in plant functional type cover across Arctic and boreal Alaska and Yukon. *Environmental Research Letters*, **17**, 054042.

Madani, N., Kimball, J.S., Ballantyne, A.P., Affleck, D.L.R., van Bodegom, P.M., Reich, P.B., Kattge, J., Sala, A., Nazeri, M., Jones, M.O., Zhao, M. & Running, S.W. (2018) Future global productivity will be affected by plant trait response to climate. *Scientific Reports*, **8**, 2870.

Maynard, D.S., Bialic-Murphy, L., Zohner, C.M., Averill, C., van den Hoogen, J., Ma, H., Mo, L., Smith, G.R., Acosta, A.T.R., Aubin, I., Berenguer, E., Boonman, C.C.F., Catford, J.A., Cerabolini, B.E.L., Dias, A.S., González-Melo, A., Hietz, P., Lusk, C.H., Mori, A.S., Niinemets, Ü., Pillar, V.D., Pinho, B.X., Rosell, J.A., Schurr, F.M., Sheremetev, S.N., da Silva, A.C., Sosinski, Ê., van Bodegom, P.M., Weiher, E., Bönisch, G., Kattge, J. & Crowther, T.W. (2022) Global relationships in tree functional traits. *Nature Communications*, **13**, 3185.

Meyer, H. & Pebesma, E. (2021) Predicting into unknown space? Estimating the area of applicability of spatial prediction models. *Methods in Ecology and Evolution*, **12**, 1620–1633.

Moreno-Martínez, Á., Camps-Valls, G., Kattge, J., Robinson, N., Reichstein, M., van Bodegom, P., Kramer, K., Cornelissen, J.H.C., Reich, P., Bahn, M., Niinemets, Ü., Peñuelas, J., Craine, J.M., Cerabolini, B.E.L., Minden, V., Laughlin, D.C., Sack, L., Allred, B., Baraloto, C., Byun, C., Soudzilovskaia, N.A. & Running, S.W. (2018) A methodology to derive global maps of leaf traits using remote sensing and climate data. *Remote Sensing of Environment*, **218**, 69–88.

Mugabowindekwe, M., Brandt, M., Chave, J., Reiner, F., Skole, D.L., Kariryaa, A., Igel, C., Hiernaux, P., Ciais, P. & Mertz, O. (2022) Nation-wide mapping of tree-level aboveground carbon stocks in Rwanda. *Nature Climate Change*, 1–7.

Oleksyn, J., Wyka, T.P., Żytkowiak, R., Zadworny, M., Mucha, J., Dering, M., Ufnalski, K., Nihlgård, B. & Reich, P.B. (2020) A fingerprint of climate change across pine forests of Sweden. *Ecology letters*, **23**, 1739–1746.

Ploton, P., Mortier, F., Réjou-Méchain, M., Barbier, N., Picard, N., Rossi, V., Dormann, C., Cornu, G., Viennois, G., Bayol, N., Lyapustin, A., Gourlet-Fleury, S. & Pélissier, R. (2020) Spatial validation reveals poor predictive performance of large-scale ecological mapping models. *Nature Communications*, **11**, 4540.

Potapov, P., Li, X., Hernandez-Serna, A., Tyukavina, A., Hansen, M.C., Kommareddy, A., Pickens, A., Turubanova, S., Tang, H., Silva, C.E., Armston, J., Dubayah, R., Blair, J.B. & Hofton, M. (2021) Mapping global forest canopy height through integration of GEDI and Landsat data. *Remote Sensing of Environment*, **253**, 112165.

Poulter, B., MacBean, N., Hartley, A., Khlystova, I., Arino, O., Betts, R., Bontemps, S., Boettcher, M., Brockmann, C., Defourny, P., Hagemann, S., Herold, M., Kirches, G., Lamarche, C., Lederer, D., Ottlé, C., Peters, M. & Peylin, P. (2015) Plant functional type classification for earth system models: results from the European Space Agency's Land Cover Climate Change Initiative. *Geoscientific Model Development*, **8**, 2315–2328.

Reich, P.B. (2014) The world-wide 'fast-slow' plant economics spectrum: a traits manifesto. *Journal of Ecology*, **102**, 275–301.

Reich, P.B., Wright, I.J. & Lusk, C.H. (2007) PREDICTING LEAF PHYSIOLOGY FROM SIMPLE PLANT AND CLIMATE ATTRIBUTES: A GLOBAL GLOPNET ANALYSIS. *Ecological Applications*, **17**, 1982–1988.

Sabatini, F.M., Lenoir, J., Hattab, T., Arnst, E.A., Chytrý, M., Dengler, J., Ruffray, P.D., Hennekens, S.M., Jandt, U., Jansen, F., Jiménez, B., Kattge, J., Levesley, A., Pillar, V.D., Purschke, O., Sandel, B., Sultana, F., Aavik, T., Aćić, S., Acosta, A.T.R., Agrillo, E., Alvarez, M., Apostolova, I., Aubin, I., Banerjee, A., Bauters, M., Bergeron, Y., Bergmeier, E., Biurrun, I., Bjorkman, A.D., Bonari, G., Bondareva, V., Brunet, J., Čarni, A., Casella, L., Cayuela, L., Černý, T., Chepinoga, V., Csiky, J., Ćušterevska, R., Bie, E.D., de Gasper, A.L., Sanctis, M.D., Dimopoulos, P., Dolezal, J., Dziuba, T., El, M.A., El, R.M., Enquist, B., Ewald, J., Fazayeli, F., Field, R., Finckh, M., Gachet, S., Galán, A., Garbolino, E., Gholizadeh, H., Giorgis, M., Golub, V., Alsos, I.G., Grytnes, A., Guerin, G.R., Gutiérrez, A.G., Haider, S., Hatim, M.Z., Hérault, B., Mendoza, G.H., Hölzel, N., Homeier, J., Hubau, W., Indreica, A., Janssen, J.A.M., Jedrzejek, B., Jentsch, A., Jürgens, N., Kącki, Z., Kapfer, J., Karger, D.N., Kavgacı, A., Kearsley, E., Kessler, M., Khanina, L., Killeen, T., Korolyuk, A., Kreft, H., Kühl, H.S., Kuzemko, A., Landucci, F., Lengyel, A., Lens, F., Lingner, D.V., Liu, H., Lysenko, T., Mahecha, M.D., Marcenò, C., Martynenko, V., Moeslund, J.E. & Mendoza, A.M. (2021) sPlotOpen – An environmentally balanced, open-access, global dataset of vegetation plots. *Global Ecology and Biogeography*, **00**, 1–25.

Scheiter, S., Langan, L. & Higgins, S.I. (2013) Next-generation dynamic global vegetation models: learning from community ecology. *New Phytologist*, **198**, 957–969.

Schiller, C., Schmidtlein, S., Boonman, C., Moreno-Martínez, A. & Kattenborn, T. (2021) Deep learning and citizen science enable automated plant trait predictions from photographs. *Scientific Reports*, **11**, 16395.

Simard, M., Pinto, N., Fisher, J.B. & Baccini, A. (2011) Mapping forest canopy height globally with spaceborne lidar. *Journal of Geophysical Research*, **116**, G04021.

Šímová, I., Violle, C., Svenning, J.-C., Kattge, J., Engemann, K., Sandel, B., Peet, R.K., Wiser, S.K., Blonder, B., McGill, B.J., Boyle, B., Morueta-Holme, N., Kraft, N.J.B., van Bodegom, P.M., Gutiérrez, A.G., Bahn, M., Ozinga, W.A., Tószögyová, A. & Enquist, B.J. (2018) Spatial patterns and climate relationships of major plant traits in the New World differ between woody and herbaceous species. *Journal of Biogeography*, **45**, 895–916.

Soetart, K., Van den Meersche, K. & van Oevelen, D. (2022) limSolve: Solving Linear Inverse Models. R package version 1.5.1. *R package*.
Swenson, N.G. & Weiser, M.D. (2010) Plant geography upon the basis of functional traits: an example from eastern North American trees. *Ecology*, **91**, 2234–2241.
Vallicrosa, H., Sardans, J., Janssens, I.A. & Penuelas, J. (2021) Global maps and factors driving forest foliar elemental composition: the importance of genetic legacy. *New Phytologist*.
Vallicrosa, H., Sardans, J., Maspons, J. & Peñuelas, J. (2022) Global distribution and drivers of forest biome foliar nitrogen to phosphorus ratios (N:P). *Global Ecology and Biogeography*, **31**, 861–871.
Van Bodegom, P.M., Douma, J.C., Witte, J.P.M., Ordoñez, J.C., Bartholomeus, R.P. & Aerts, R. (2012) Going beyond limitations of plant functional types when predicting global ecosystem-atmosphere fluxes: exploring the merits of traits-based approaches: Merits of traits-based vegetation modelling. *Global Ecology and Biogeography*, **21**, 625–636.
Van den Meersche, K., Soetaert, K. & Van Oevelen, D. (2009) xsample (): an R function for sampling linear inverse problems. *Journal of Statistical Software*, **30**, 1–15.
Walker, A.P., Beckerman, A.P., Gu, L., Kattge, J., Cernusak, L.A., Domingues, T.F., Scales, J.C., Wohlfahrt, G., Wullschleger, S.D. & Woodward, F.I. (2014) The relationship of leaf photosynthetic traits - V_{cmax} and J_{max} - to leaf nitrogen, leaf phosphorus, and specific leaf area: a meta-analysis and modeling study. *Ecology and Evolution*, **4**, 3218–3235.
Walker, A.P., Quaife, T., van Bodegom, P.M., De Kauwe, M.G., Keenan, T.F., Joiner, J., Lomas, M.R., MacBean, N., Xu, C., Yang, X. & Woodward, F.I. (2017) The impact of alternative trait-scaling hypotheses for the maximum photosynthetic carboxylation rate (V_{cmax}) on global gross primary production. *New Phytologist*, **215**, 1370–1386.
Wang, H., Harrison, S.P., Li, M., Prentice, I.C., Qiao, S., Wang, R., Xu, H., Mengoli, G., Peng, Y. & Yang, Y. (2022a) The China plant trait database version 2. *Scientific Data*, **9**, 769.
Wang, L., Arora, V.K., Bartlett, P., Chan, E. & Curasi, S.R. (2022b) *Mapping of ESA-CCI land cover data to plant functional types for use in the CLASSIC land model*, Biogeochemistry: Modelling, Terrestrial.
Wang, W., Fan, Y., Li, Y., Li, X. & Tang, S. (2023) An Individual Tree Segmentation Method from Mobile Mapping Point Clouds Based on Improved 3D Morphological Analysis. *IEEE Journal of Selected Topics in Applied Earth Observations and Remote Sensing*.
Wang, Y., Li, G., Ding, J., Guo, Z., Tang, S., Wang, C., Huang, Q., Liu, R. & Chen, J.M. (2016) A combined GLAS and MODIS estimation of the global distribution of mean forest canopy height. *Remote Sensing of Environment*, **174**, 24–43.
Wang, Z., Chlus, A., Geygan, R., Ye, Z., Zheng, T., Singh, A., Couture, J.J., Cavender-Bares, J., Kruger, E.L. & Townsend, P.A. (2020) Foliar functional traits from imaging spectroscopy across biomes in eastern North America. *New Phytologist*, nph.16711.
Wolf, S., Mahecha, M.D., Sabatini, F.M., Wirth, C., Bruelheide, H., Kattge, J., Moreno Martínez, Á., Mora, K. & Kattenborn, T. (2022) Citizen science plant observations encode global trait patterns. *Nature Ecology & Evolution*.
Wright, I.J., Reich, P.B., Cornelissen, J.H.C., Falster, D.S., Garnier, E., Hikosaka, K., Lamont, B.B., Lee, W., Oleksyn, J., Osada, N., Poorter, H., Villar, R., Warton, D.I. & Westoby, M. (2005) Assessing the generality of global leaf trait relationships. *New Phytologist*, **166**, 485–496.
Wright, I.J., Reich, P.B., Westoby, M., Ackerly, D.D., Baruch, Z., Bongers, F., Cavender-Bares, J., Chapin, T., Cornelissen, J.H.C., Diemer, M., Flexas, J., Garnier, E., Groom, P.K., Gulias, J., Hikosaka, K., Lamont, B.B., Lee, T., Lee, W., Lusk, C., Midgley, J.J. & Navas, M.-L. (2004) The worldwide leaf economics spectrum. **428**, 7.
Wu, J. (2007) *Scale and scaling: a cross-disciplinary perspective*. *Key topics in landscape ecology*, pp. 115–142. Cambridge University Press.
Yang, Y., Zhu, Q., Peng, C., Wang, H. & Chen, H. (2015) From plant functional types to plant functional traits: A new paradigm in modelling global vegetation dynamics. *Progress in Physical Geography: Earth and Environment*, **39**, 514–535.

Yu, W., Li, J., Liu, Q., Zeng, Y., Zhao, J., Xu, B. & Yin, G. (2018) Global Land Cover Heterogeneity Characteristics at Moderate Resolution for Mixed Pixel Modeling and Inversion. *Remote Sensing*, **10**, 856.

Zeng, Y., Hao, D., Huete, A., Dechant, B., Berry, J., Chen, J.M., Joiner, J., Frankenberg, C., Bond-Lamberty, B. & Ryu, Y. (2022) Optical vegetation indices for monitoring terrestrial ecosystems globally. *Nature Reviews Earth & Environment*, **3**, 477–493.

Zhang, Y.-W., Guo, Y., Tang, Z., Feng, Y., Zhu, X., Xu, W., Bai, Y., Zhou, G., Xie, Z. & Fang, J. (2021) Patterns of nitrogen and phosphorus pools in terrestrial ecosystems in China. *Earth System Science Data*, **13**, 5337–5351.